Couplings and properties measurements (Spin/Parity, mass and width) with ATLAS + CMS in bosonic Higgs decay modes

Hongtao Yang (LBNL)

on behalf of the ATLAS and CMS Collaborations

7th Edition of the Large Hadron Collider Physics Conference, Puebla, Mexico

May 20, 2019

Introduction

- Higgs boson plays a fundamental role in the Standard Model (SM)
- Bosonic decay channels ($H \rightarrow \gamma\gamma$, ZZ, WW) have excellent sensitivities at LHC
  - Leading channels for Higgs boson discovery
  - Crucial for high precision Higgs boson property measurements
- This presentation: latest ATLAS & CMS Run 2 Higgs boson property measurement results in bosonic decay channels

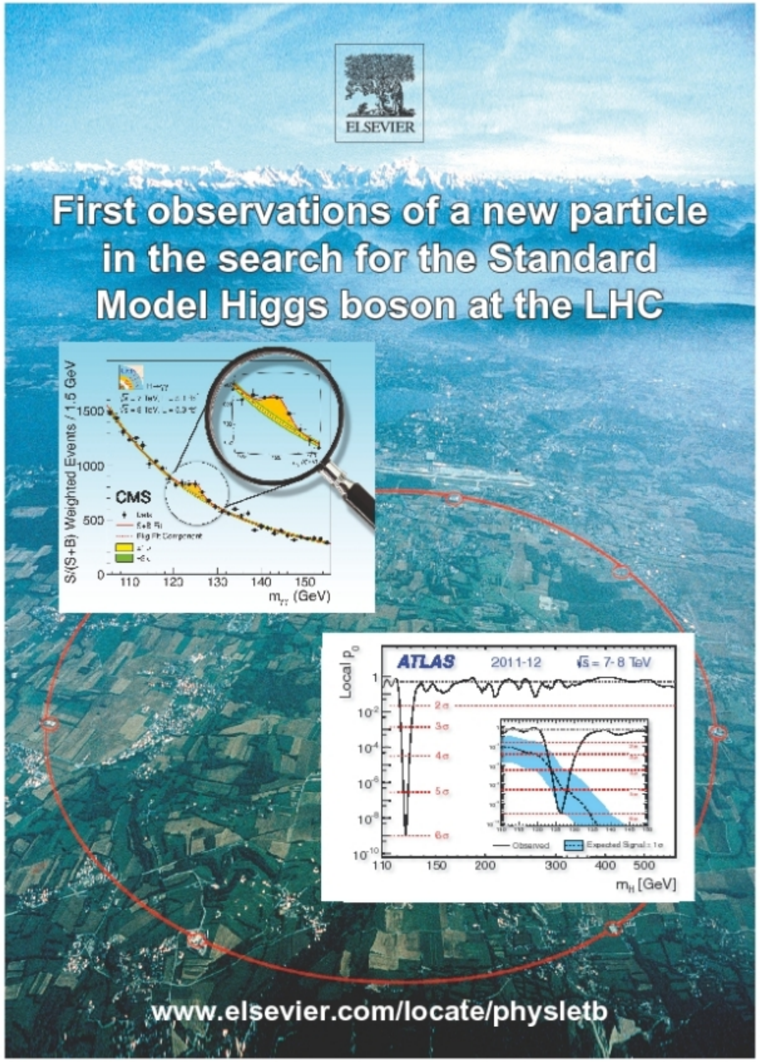

** Results labeled as "new" in this presentation are produced after LHCP2018*

Bosonic channels @ 13 TeV

m_H = 125.09 GeV (Run 1 ATLAS+CMS)	H→γγ	H→ZZ→4l	H→WW→lνlν
BR [%]	0.23	0.013	0.98
N(Higgs) in 1 fb^{-1} of pp collisions at 13 TeV	130	7	550

~56k Higgs boson produced in every fb^{-1} of 13 TeV data

H→VV

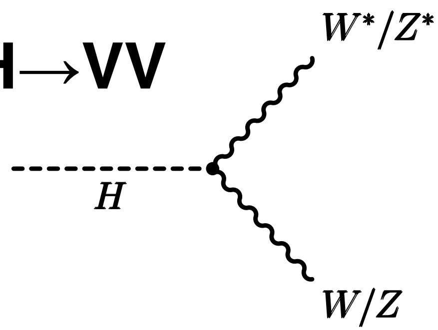

- **Small BRs!** For WW and ZZ, stick to leptonic (e, μ) decay of vector boson to suppress large bkg.
- γγ and ZZ→4l can reconstruct Higgs boson invariant mass with high resolution
- WW→lνlν has MET in the final states: rely on other observables (m_T, m_{ll} etc.)

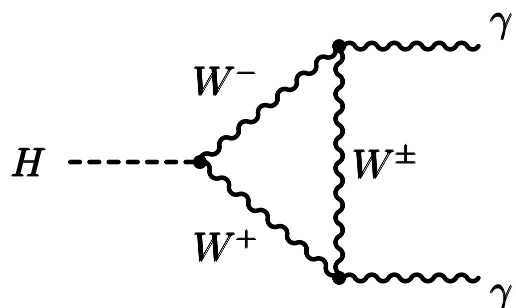

H→γγ

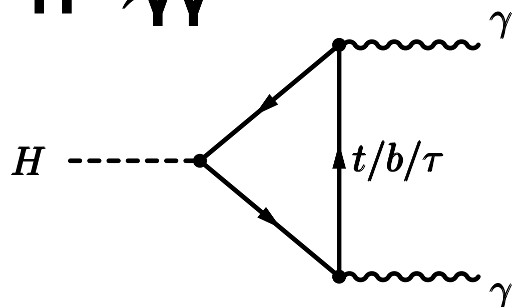

Coupling measurements

This talk will focus on ggF and VBF production modes

VH results will be covered by L. Mastrolorenzo

ttH results will be covered by J. Keller

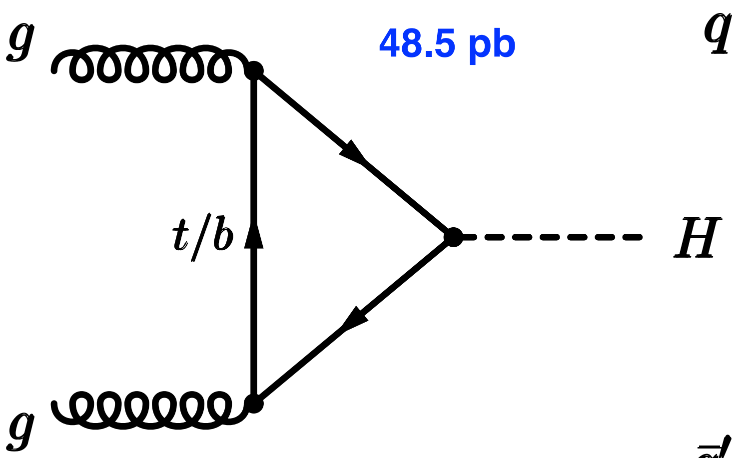

Gluon-fusion
ggF (~87%)

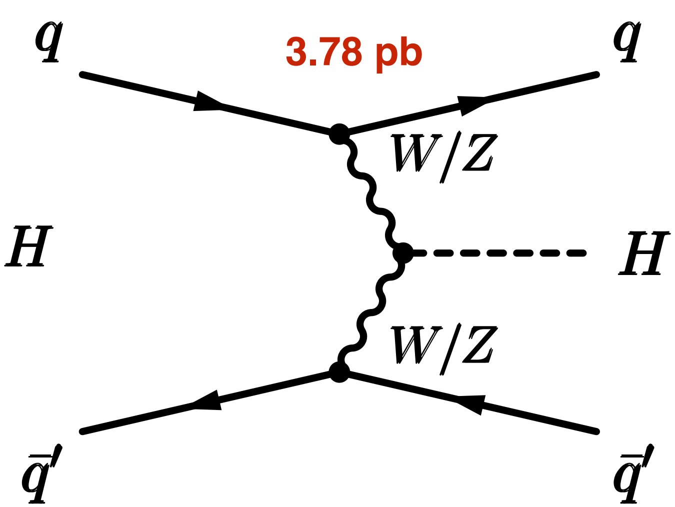

Vector boson
fusion (VBF) (~7%)

Run 2 dataset in each channel

H→γγ

ATLAS-CONF-2018-028 — Up to 2017

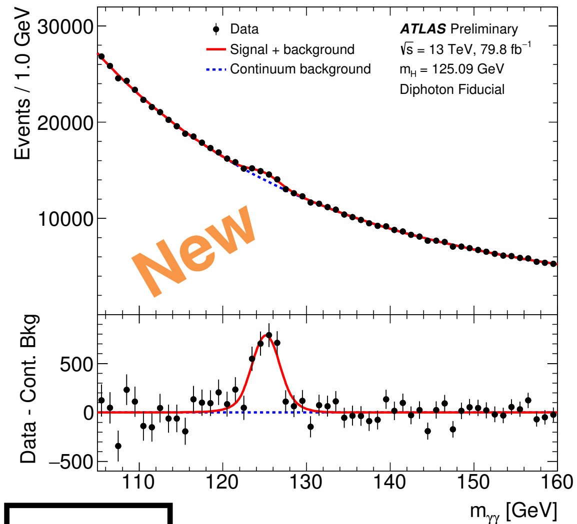

Up to 2017

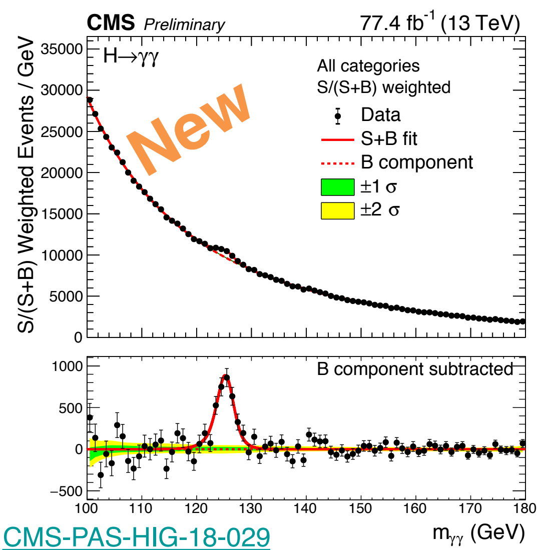

CMS-PAS-HIG-18-029

H→ZZ→4l

ATLAS-CONF-2018-018 — Up to 2017

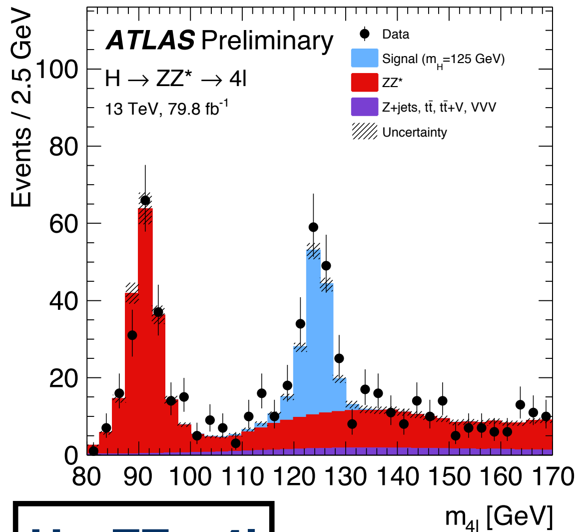

Full Run 2

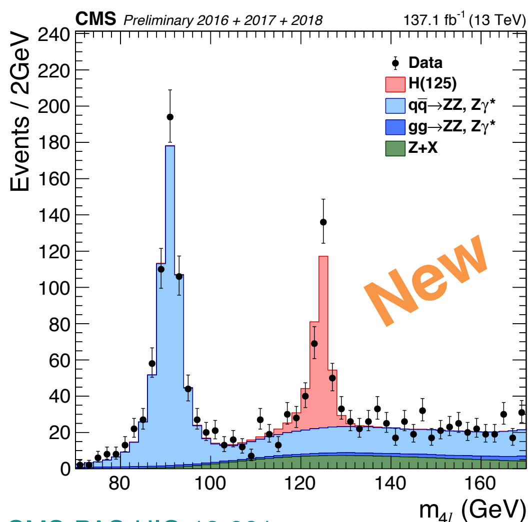

CMS-PAS-HIG-19-001

H→WW→lνlν

PLB 789 (2019) 508 — Up to 2016

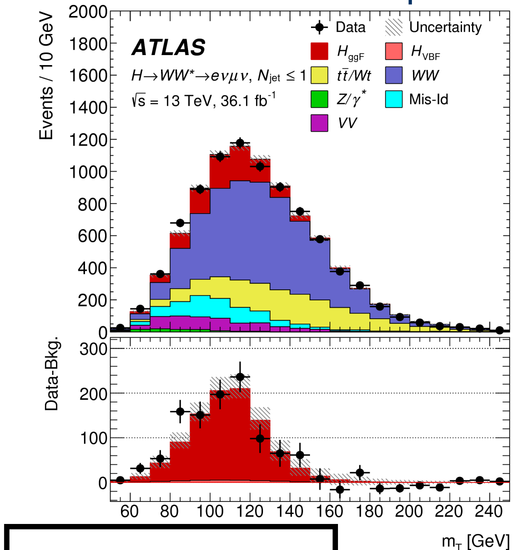

Up to 2016

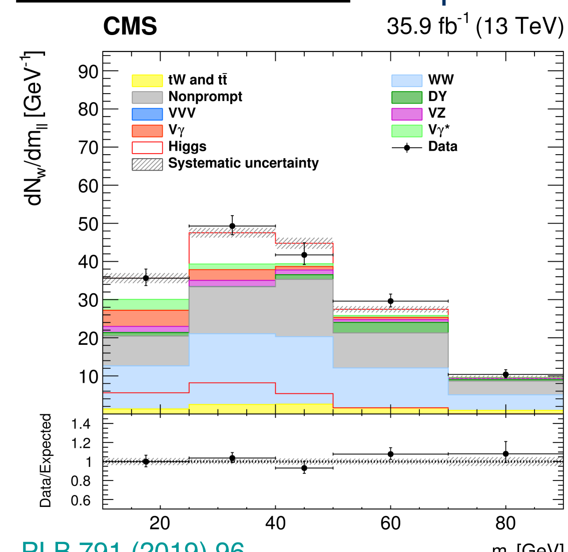

PLB 791 (2019) 96

Simplified template cross-section (STXS)

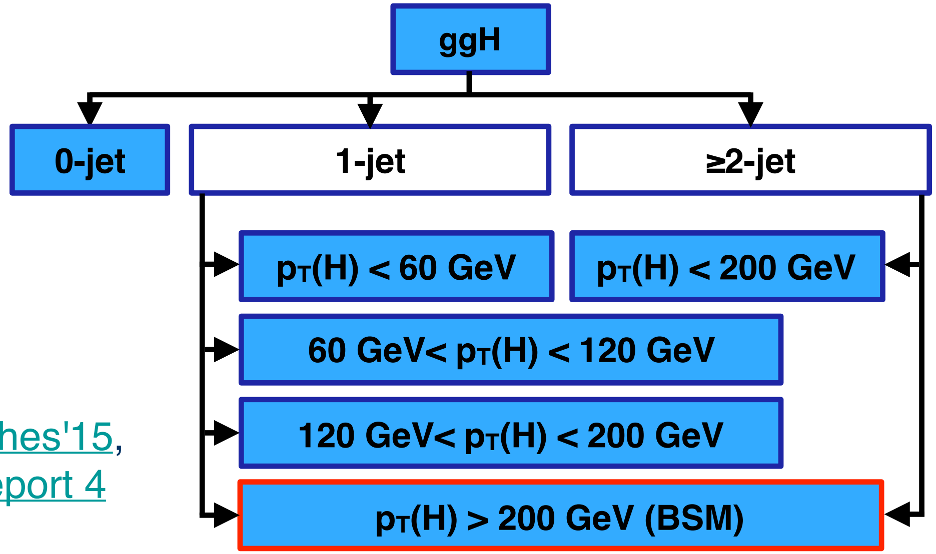

Les Houches'15, Yellow Report 4

- **Measure cross-section per production mode in different phase-space regions (more discussions in C. Kato's talk)**
  - Reduce model dependence and maximize sensitivity to BSM effects
  - Support kinematic-dependent interpretations (EFT etc.)
- Within each region, use the SM predicted signal templates to fit data
  - Can still exploit powerful analysis techniques (e.g. MVA)

H→γγ inclusive production cross-sections & STXS

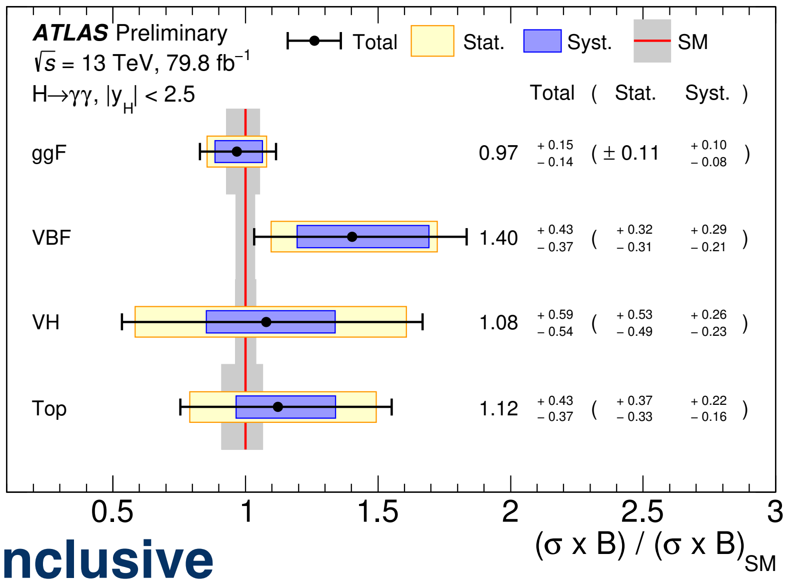

Inclusive

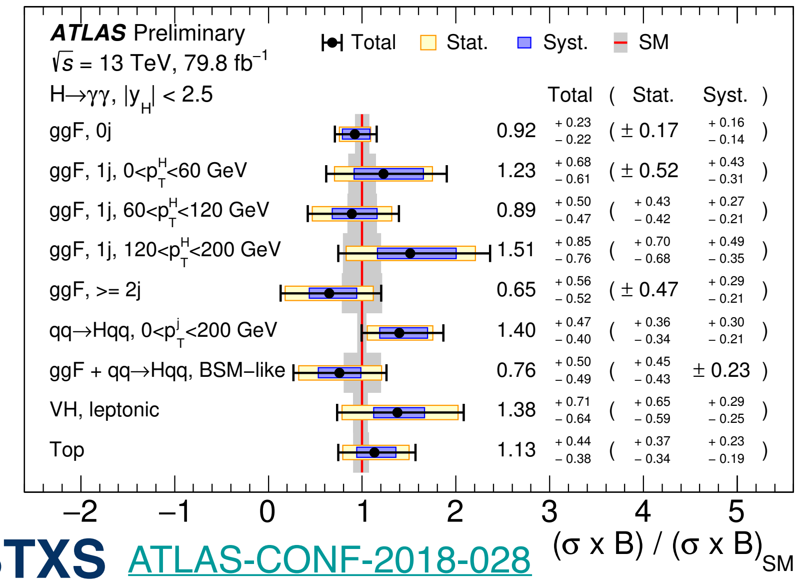

STXS

ATLAS-CONF-2018-028

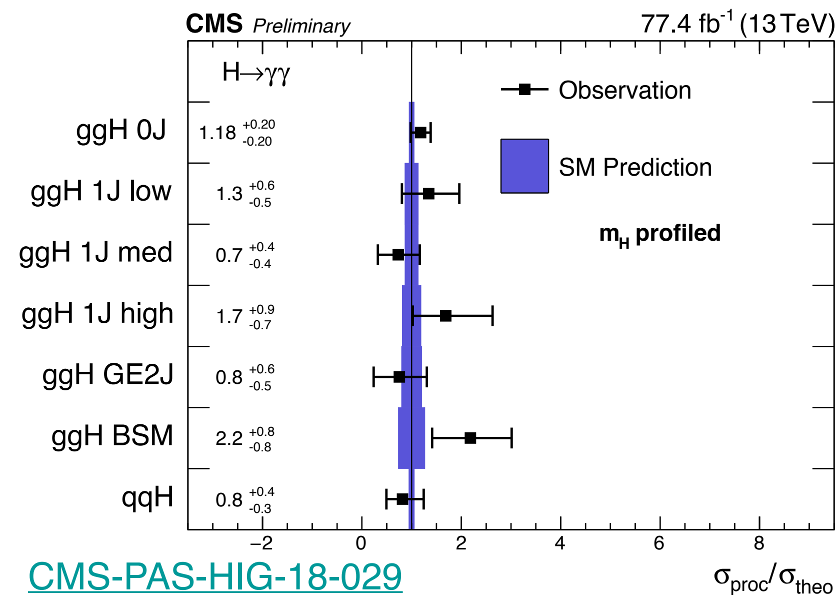

CMS-PAS-HIG-18-029

- Reaching 15% level precision for inclusive ggF cross-section, 30~40% level for VBF with ~80 fb^{-1}
- Data in good agreement with SM within uncertainties

H→ZZ→4l: inclusive production cross-sections

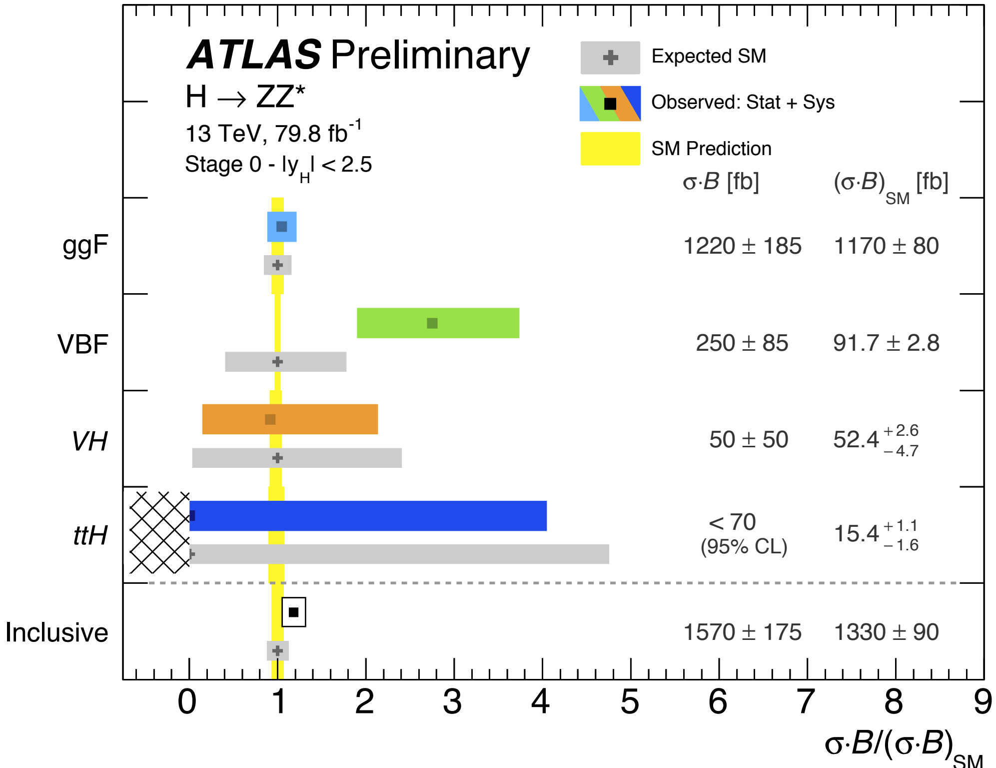

ATLAS-CONF-2018-018

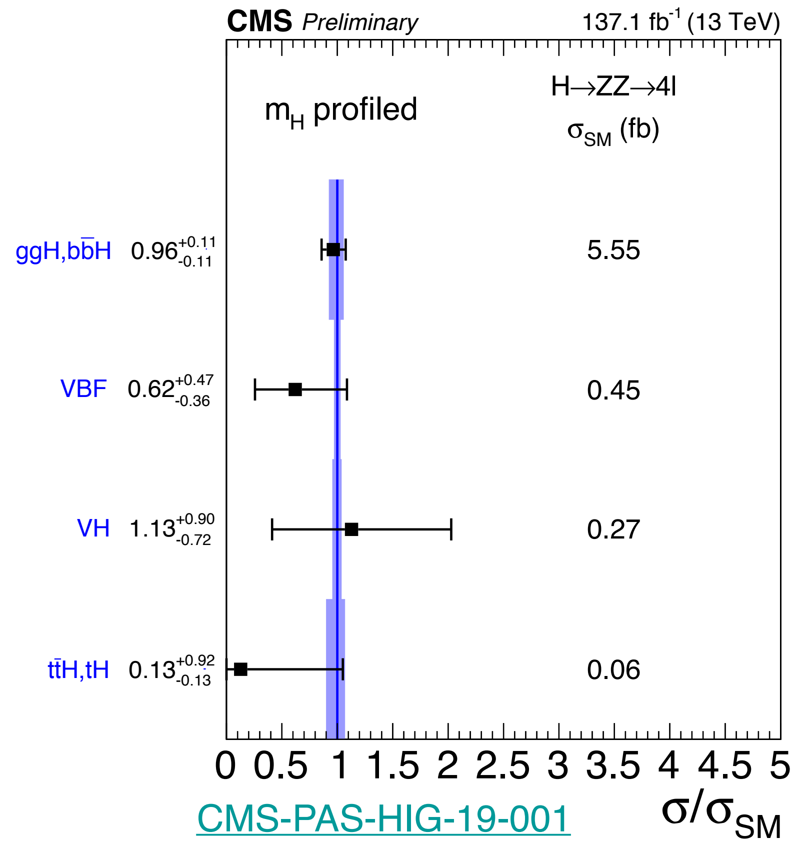

CMS-PAS-HIG-19-001

- Reaching 10% precision for ggF with full Run 2 stats
- Good agreement with SM. 2σ tension from SM in ATLAS VBF result not confirmed by CMS

H→ZZ→4l: STXS cross-sections

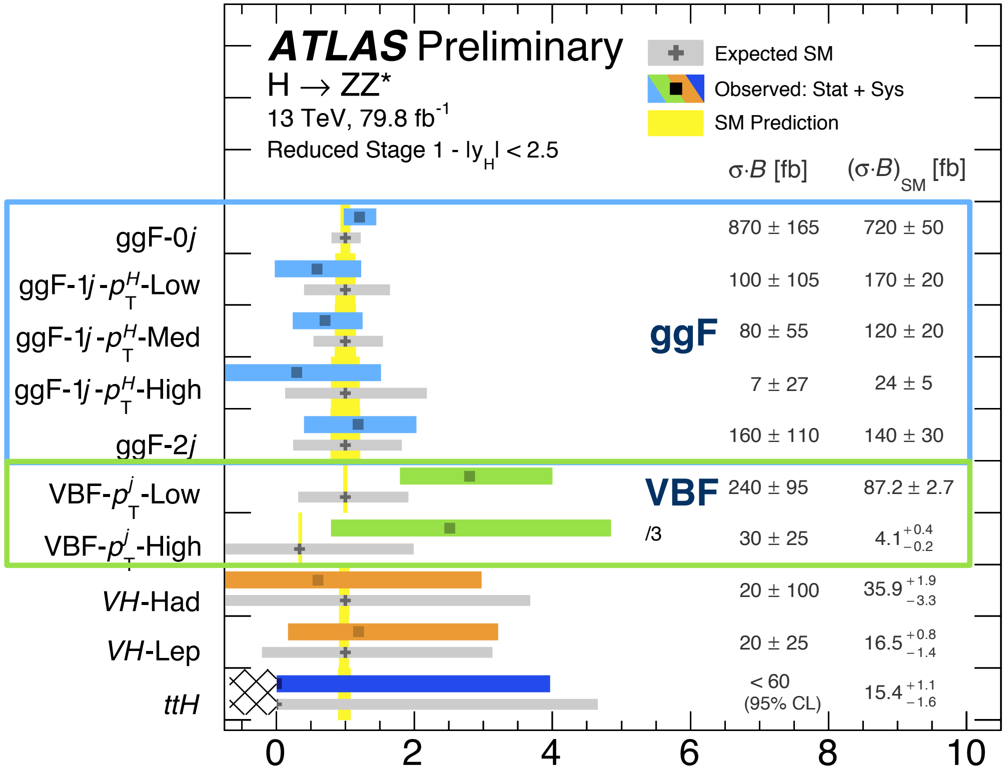

ATLAS-CONF-2018-018

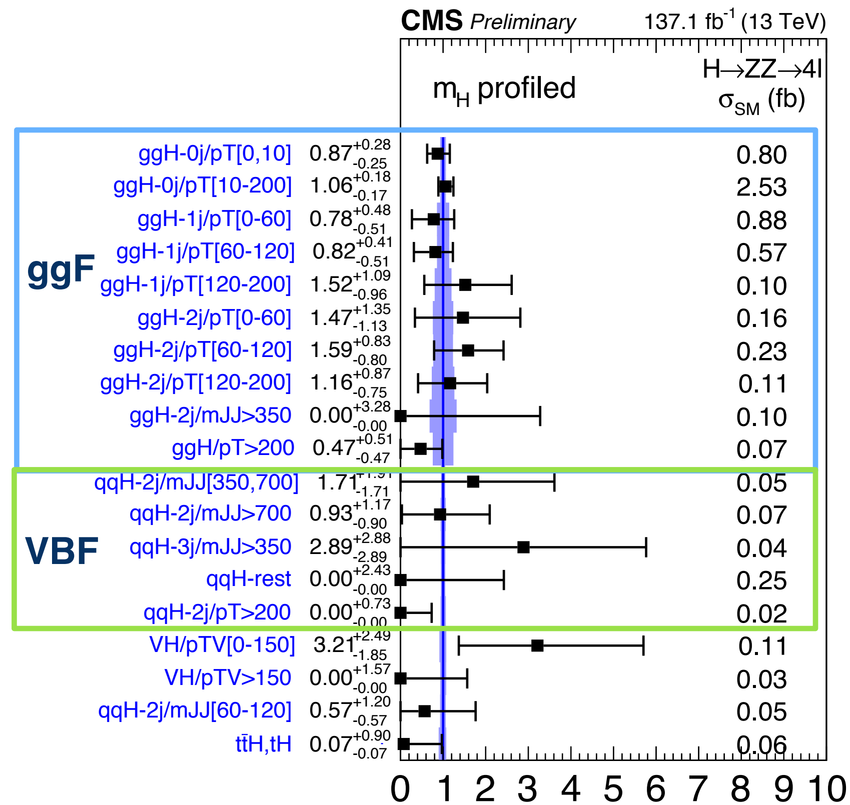

CMS-PAS-HIG-19-001

- CMS use “Stage 1.1”. Current ATLAS results based on “Stage 1” granularity (will move to “Stage 1.1” in the next step)
- Choice of binning: balance between granularity and sensitivity/correlation

H→WW→lνlν

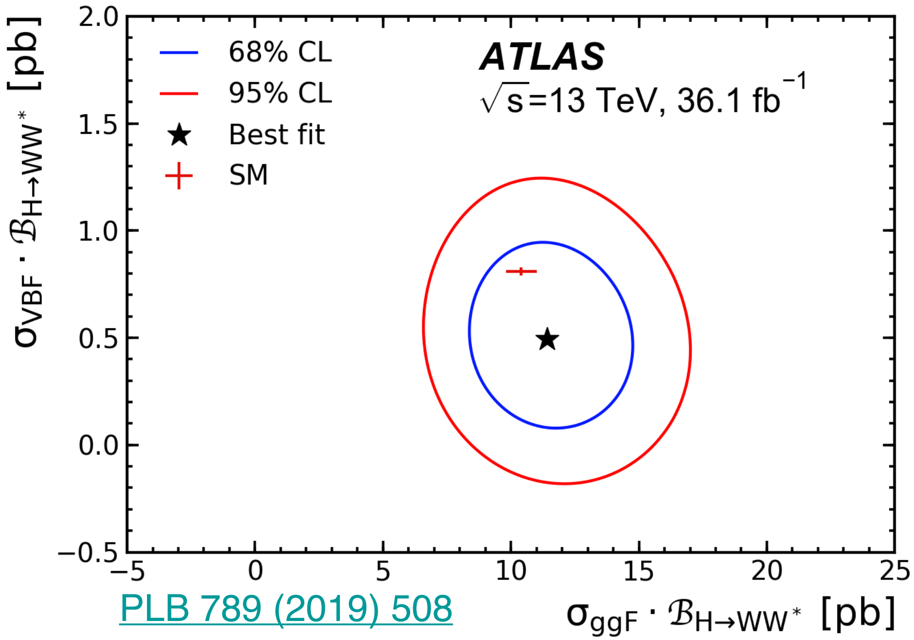

PLB 789 (2019) 508

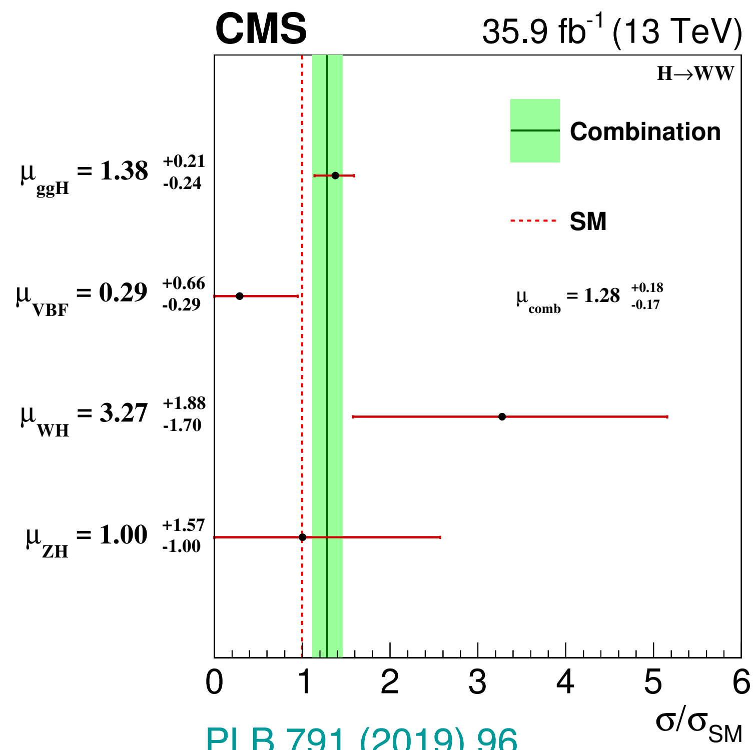

PLB 791 (2019) 96

$$\mu_{ggF} = 1.10^{+0.10}_{-0.09}(\text{stat})^{+0.13}_{-0.11}(\text{theory})^{+0.14}_{-0.13}(\text{exp})$$

$$\mu_{VBF} = 0.62^{+0.29}_{-0.27}(\text{stat})^{+0.12}_{-0.13}(\text{theory}) \pm 0.15(\text{exp})$$

- Good sensitivity for ggF (20% level precision) and VBF (50% level precision) with ~36 fb^{-1} (about a quarter of full Run 2 data)
- Two processes well separated, yielding small correlation between them

Mass, width, and CP results

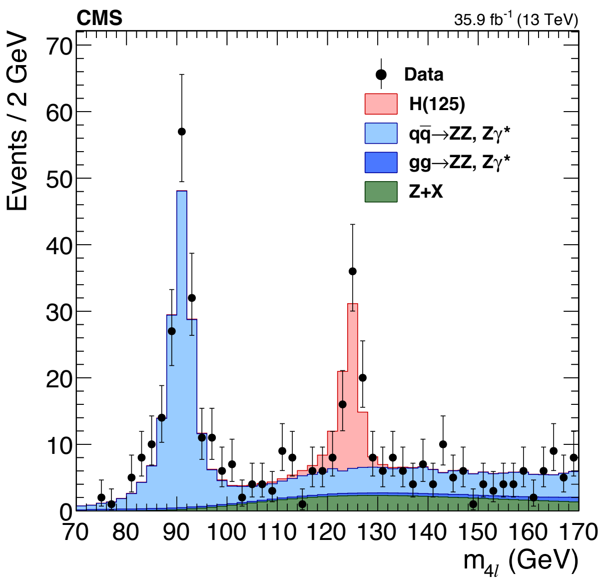

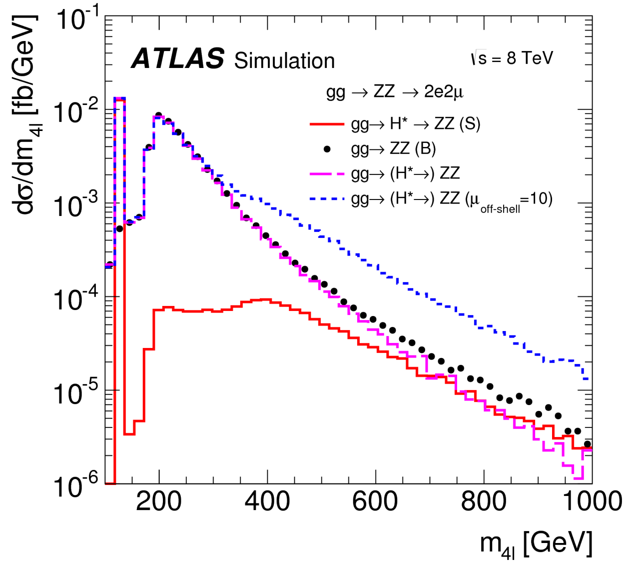

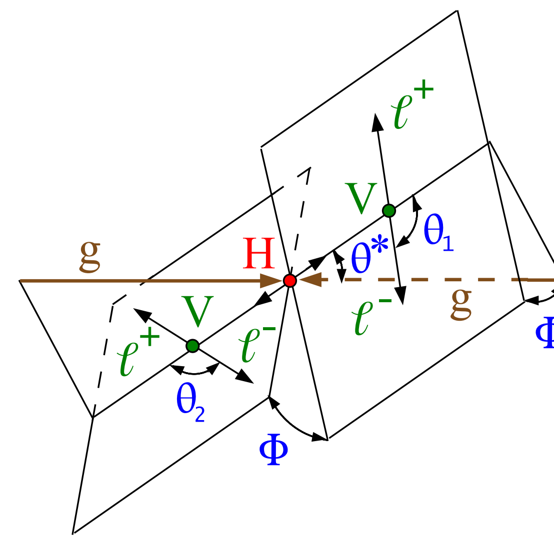

Higgs boson mass measurement

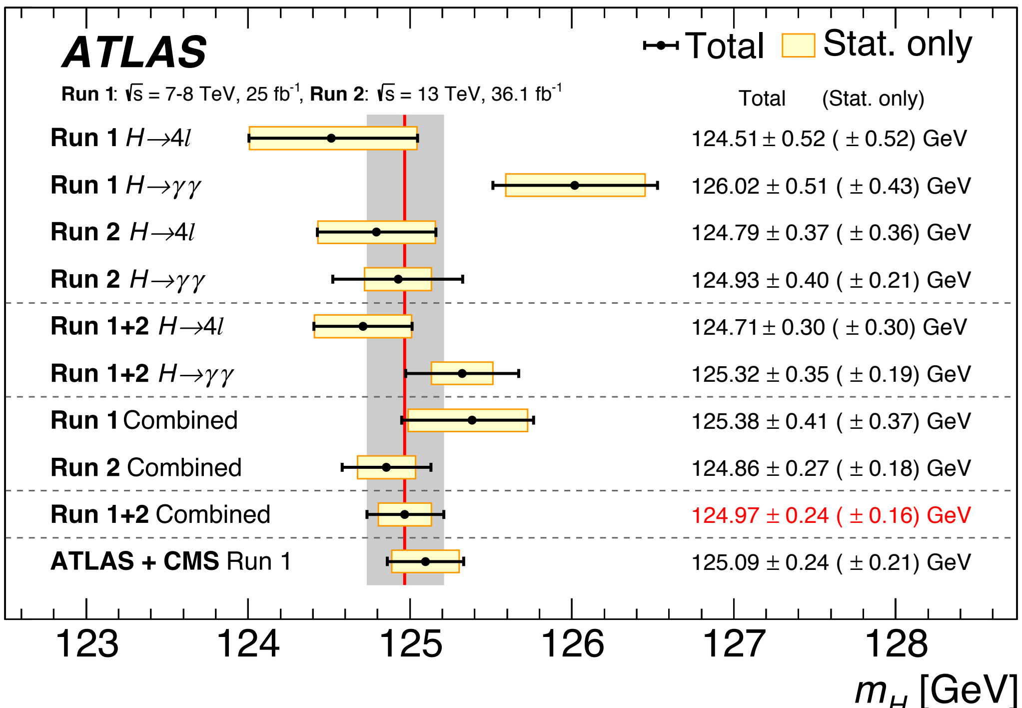

PLB 784 (2018) 345

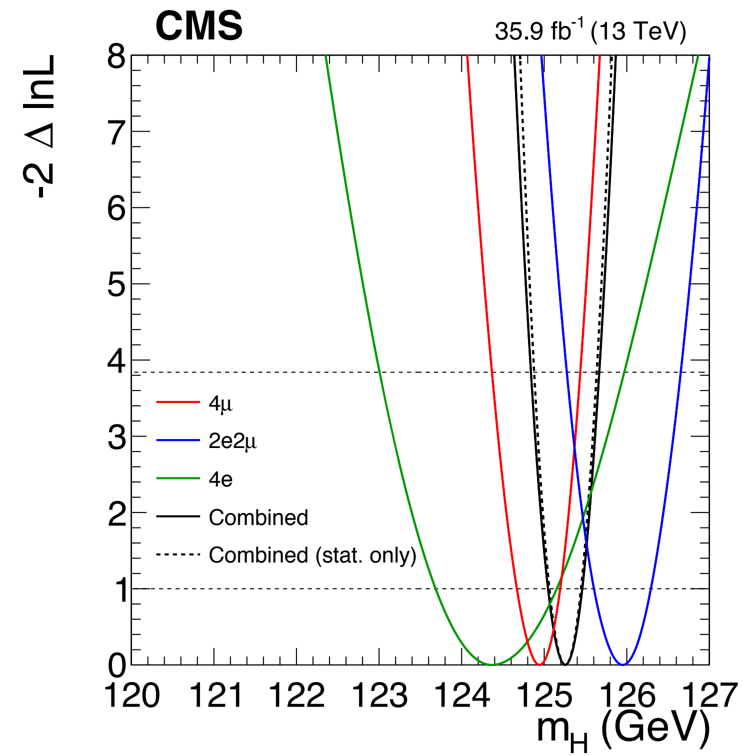

JHEP 11 (2017) 047

- ATLAS (γγ+4l): m_H = 124.97 ± 0.16 (stat.) ± 0.18 (syst.) GeV
- CMS (4l): m_H = 125.26 ± 0.20 (stat.) ± 0.08 (syst.) GeV
- Syst. uncertainty dominated by experimental ones (energy/momentum scale and resolution)

Off-shell analysis (new)

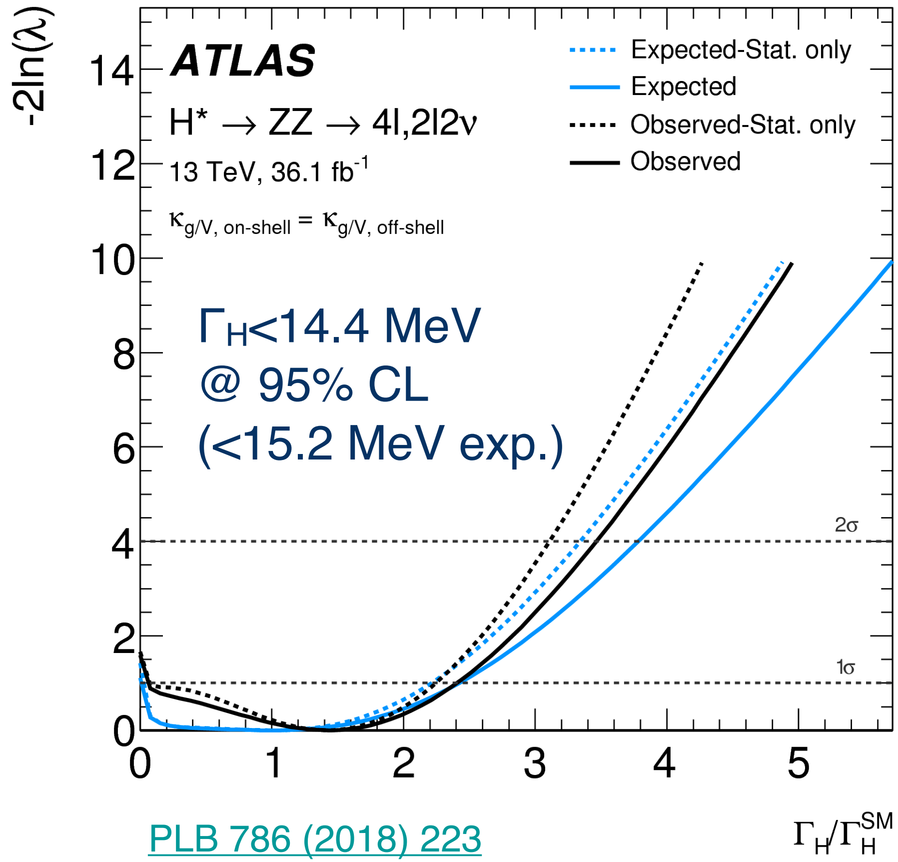

PLB 786 (2018) 223

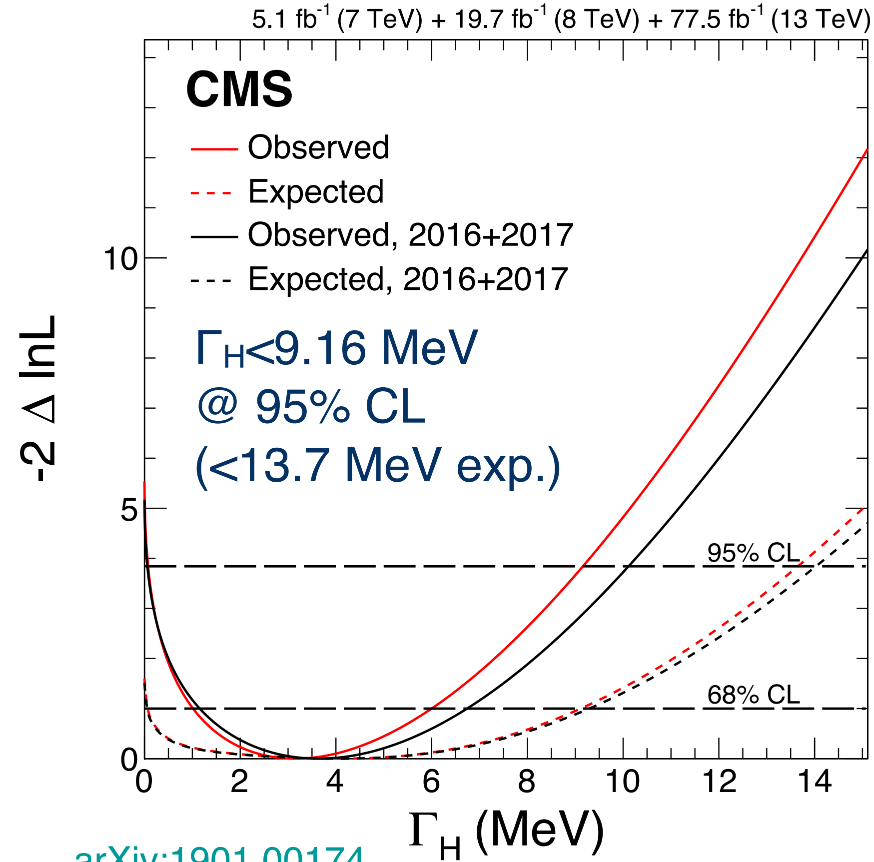

arXiv:1901.00174

- **Γ_H^{SM}=4 MeV** for m_H = 125.09 GeV: far below detector resolution!
- Use off-shell production in H→ZZ→4l/llvv channels to constrain Higgs boson total width, assuming same couplings for on-shell/off-shell regions

CP studies: CMS results

new

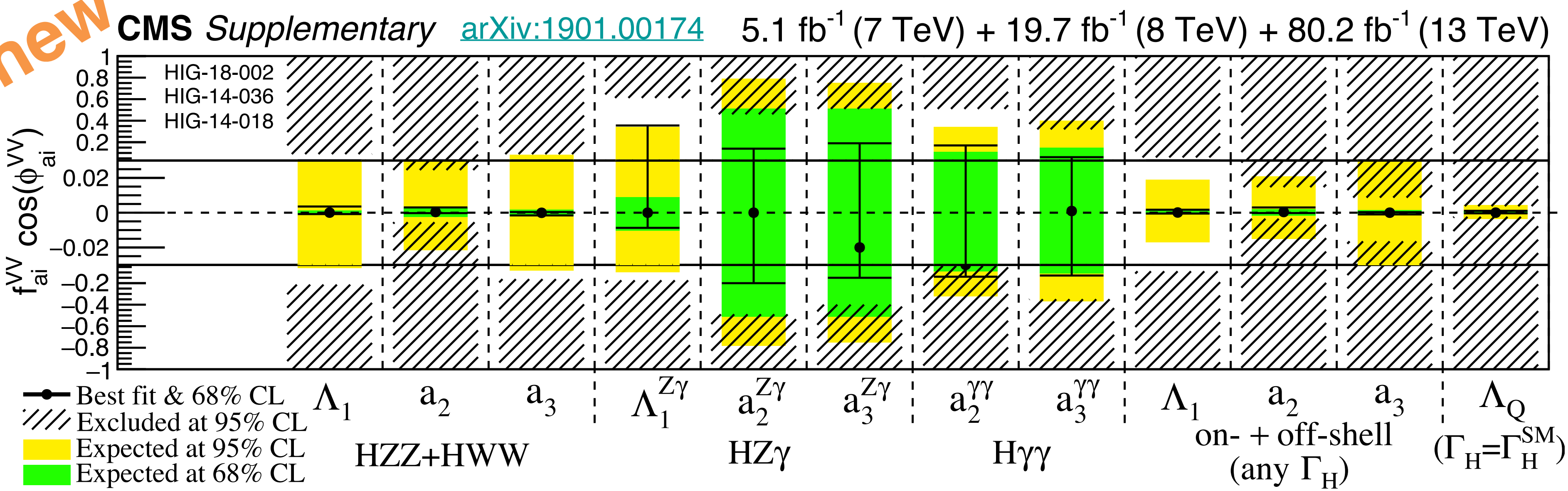

$$A \sim \left[a_1^{VV} - \frac{\kappa_1^{VV} q_1^2 + \kappa_2^{VV} q_2^2}{(\Lambda_1^{VV})^2} - \frac{\kappa_3^{VV}(q_1+q_2)^2}{(\Lambda_Q^{VV})^2}\right] m_V^2 \epsilon_{V1}^* \epsilon_{V2}^* + a_2^{VV} f_{\mu\nu}^{*(1)} f^{*(2)\mu\nu} + a_3^{VV} f_{\mu\nu}^{*(1)} \tilde{f}^{*(2)\mu\nu}$$

Leading momentum expansion

CP even

CP odd

- Spin-0 nature established in Run 1
- CP admixture as well as other BSM interactions still possible: use Run 2 data to study HVV couplings

CP studies: ATLAS results

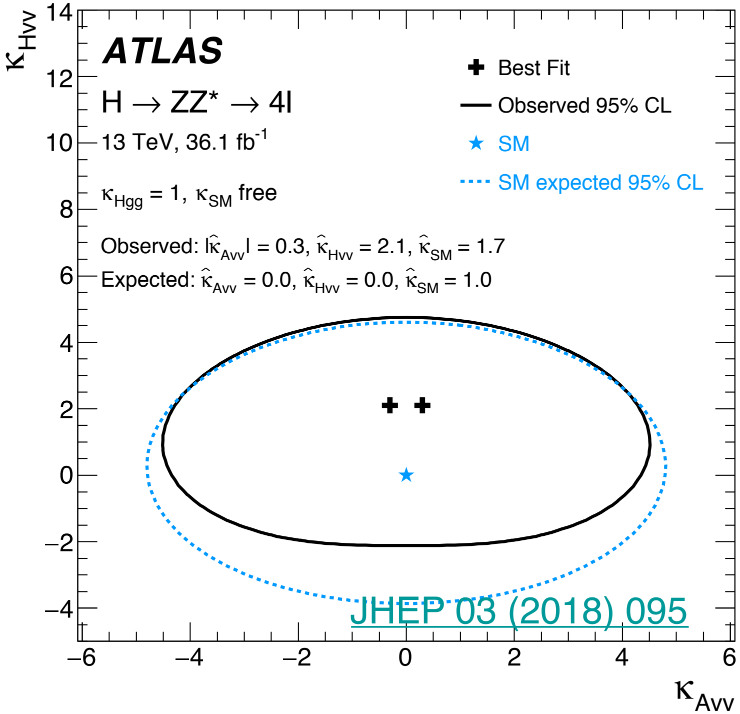

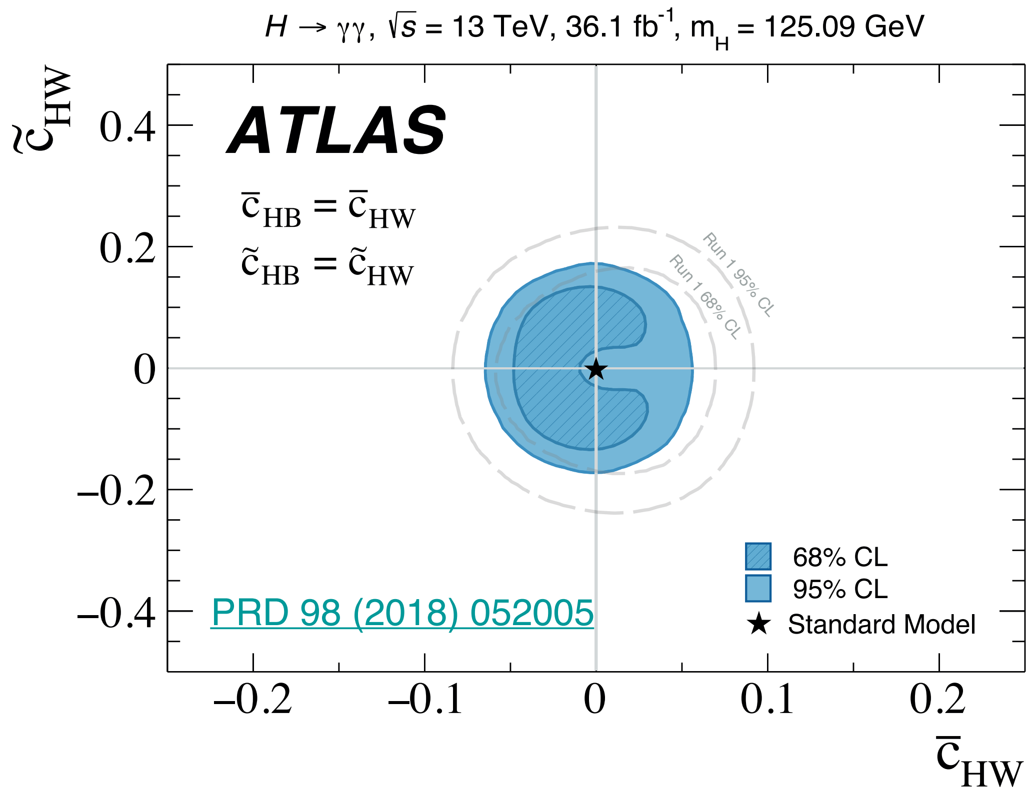

- ATLAS use Higgs characterization model or Wilson coefficients etc. to probe CP even and odd BSM interactions

Conclusions

- Bosonic decay channels continue leading Run 2 measurements of ggF (reaching 10% precision) and VBF (reaching 30% level precision) cross-sections
  - Also measured phase-space regions within production modes using STXS framework
- Higgs boson mass measurement updated with Run 2 data
- Off-shell analysis (for total width) and HVV CP studies did not show deviation from SM
- Many analyses to be updated to full Run 2 dataset, ATLAS and CMS dataset to be combined. Stay tuned for more results!

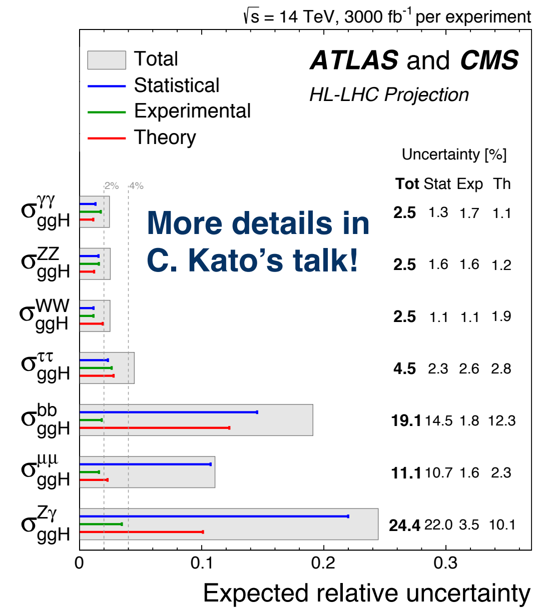

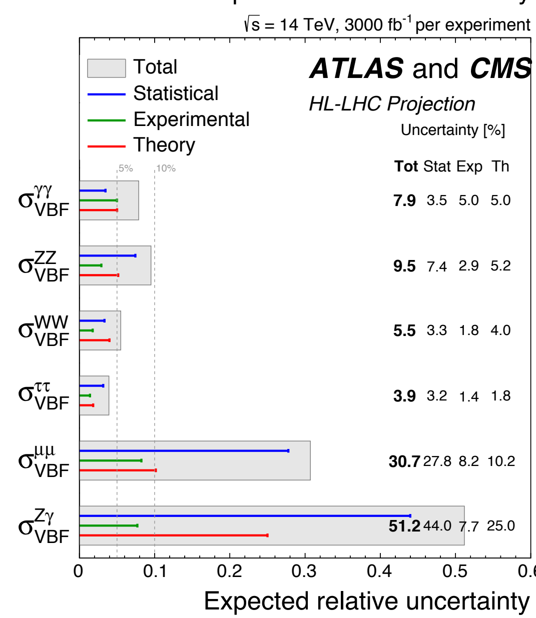

References

- LHC Higgs Cross-section Working Group, "Handbook of LHC Higgs Cross Sections: 4. Deciphering the Nature of the Higgs Sector", arXiv:1610.07922
- ATLAS Collaboration, "Measurements of Higgs boson properties in the diphoton decay channel using 80 fb^{-1} of pp collision data at $\sqrt{s}$ = 13 TeV with the ATLAS detector", ATLAS-CONF-2018-028
- ATLAS Collaboration, "Measurements of the Higgs boson production, fiducial and differential cross sections in the 4ℓ decay channel at $\sqrt{s}$ = 13 TeV with the ATLAS detector", ATLAS-CONF-2018-018
- ATLAS Collaboration, "Measurements of gluon-gluon fusion and vector-boson fusion Higgs boson production cross-sections in the $H \to WW^* \to e\nu\mu\nu$ decay channel in pp collisions at $\sqrt{s}$ = 13 TeV with the ATLAS detector", PLB 789 (2019) 508
- ATLAS Collaboration, "Measurement of the Higgs boson mass in the $H \to ZZ^* \to 4\ell$ and $H \to \gamma\gamma$ channels with $\sqrt{s}$ = 13 TeV pp collisions using the ATLAS detector", PLB 784 (2018) 345
- ATLAS Collaboration, "Constraints on off-shell Higgs boson production and the Higgs boson total width in $ZZ \to 4\ell$ and $ZZ \to 2\ell 2\nu$ final states with the ATLAS detector", PLB 786 (2018) 223
- Measurements of Higgs boson properties in the diphoton decay channel with 36 fb^{-1} of pp collision data at $\sqrt{s}$ = 13 TeV with the ATLAS detector, PRD 98 (2018) 052005
- ATLAS Collaboration, "Measurement of the Higgs boson coupling properties in the $H \to ZZ^* \to 4\ell$ decay channel at $\sqrt{s}$ = 13 TeV with the ATLAS detector", JHEP 03 (2018) 095
- CMS Collaboration, "Measurements of Higgs boson production via gluon fusion and vector boson fusion in the diphoton decay channel at $\sqrt{s}$ = 13 TeV", CMS-PAS-HIG-18-029
- CMS Collaboration, "Measurements of properties of the Higgs boson in the four-lepton final state in proton-proton collisions at $\sqrt{s}$ = 13 TeV", CMS-PAS-HIG-19-001
- CMS Collaboration, "Measurements of properties of the Higgs boson decaying to a W boson pair in pp collisions at $\sqrt{s}$ = 13 TeV", PLB 791 (2019) 96
- CMS Collaboration, "Measurements of properties of the Higgs boson decaying into the four-lepton final state in pp collisions at $\sqrt{s}$ = 13 TeV", JHEP 11 (2017) 047
- CMS Collaboration, "Measurements of the Higgs boson width and anomalous HVV couplings from on-shell and off-shell production in the four-lepton final state", arXiv:1901.00174, accepted by PRD

Backup

LHC and ATLAS detector

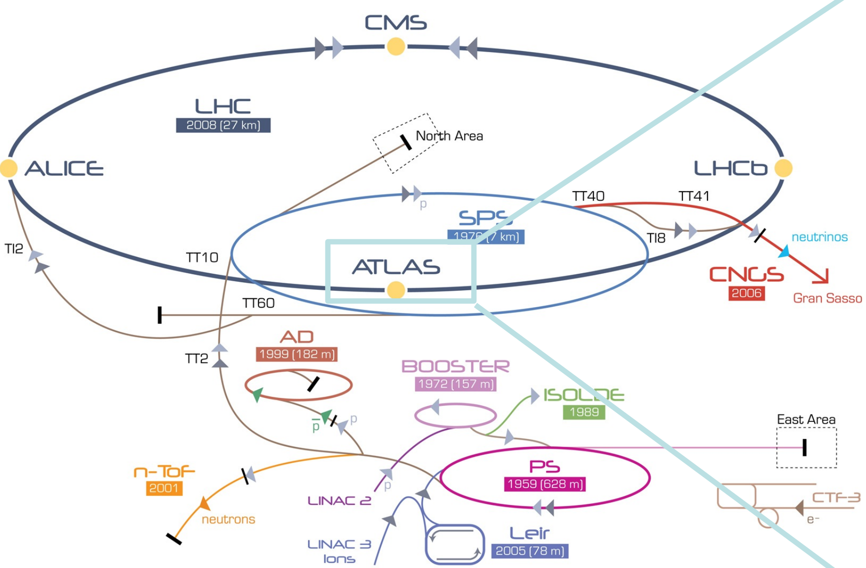

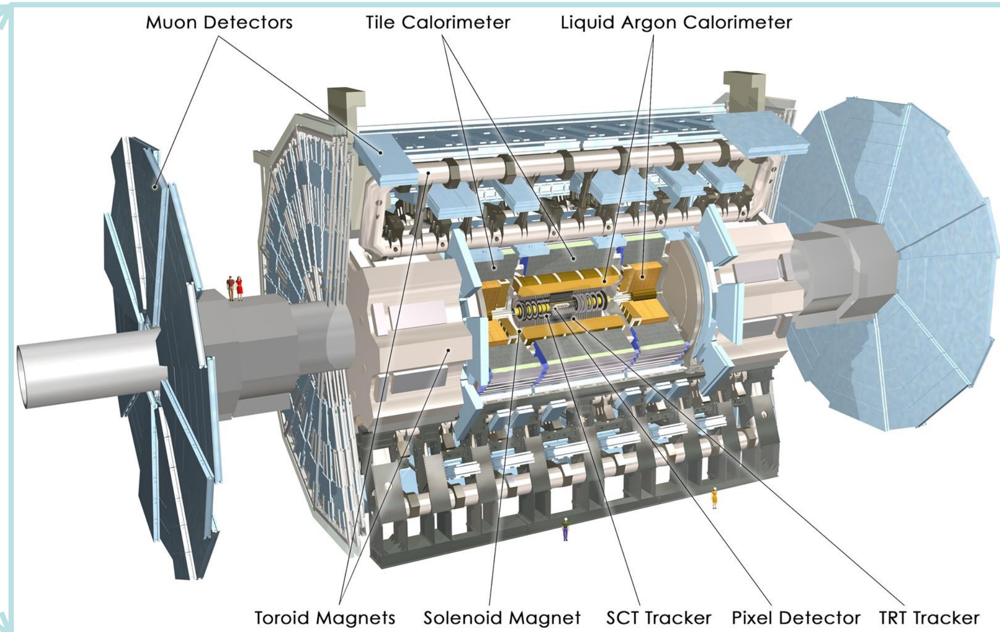

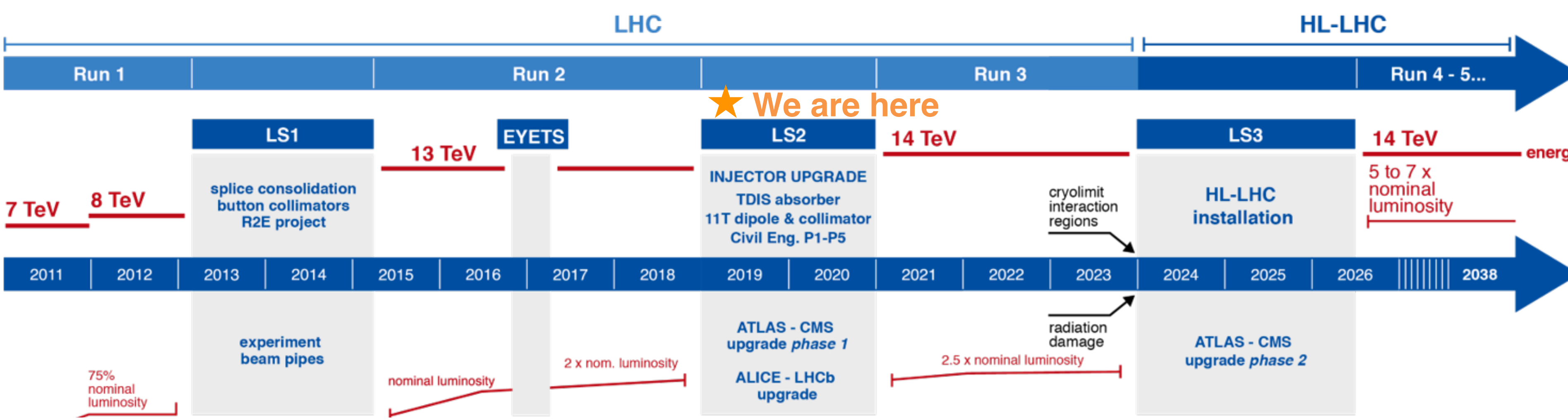

SM Higgs boson production at LHC

Main

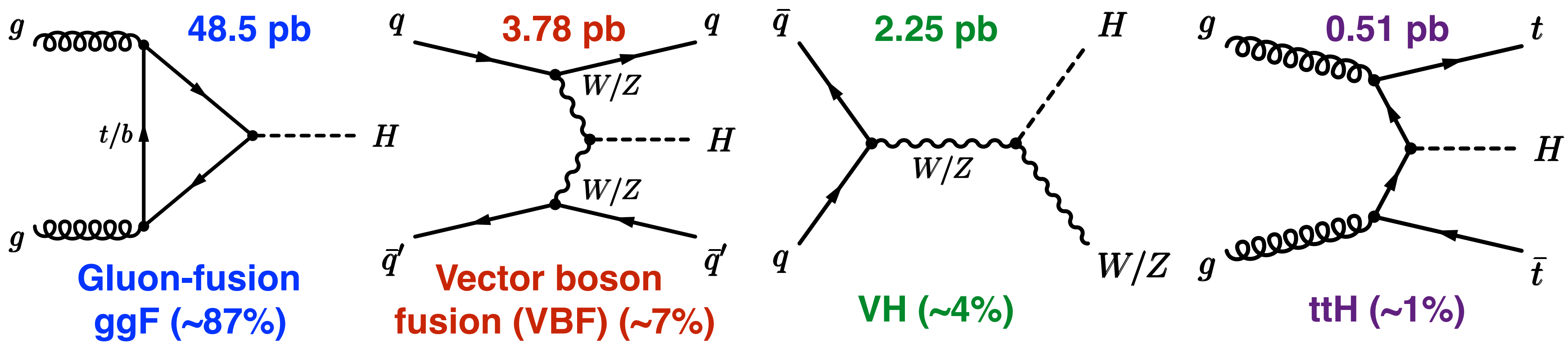

Rare

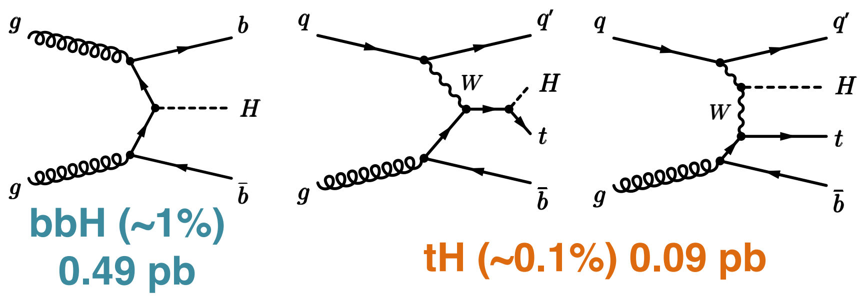

- Distinct topology from each production mode
- Rare production modes difficult to probe, but important for beyond the SM (BSM) scenarios
- Improved accuracy from theory calculations: inclusive σ(ggF) now calculated at N^{3}LO in QCD and NLO in EW, with 5% uncertainty

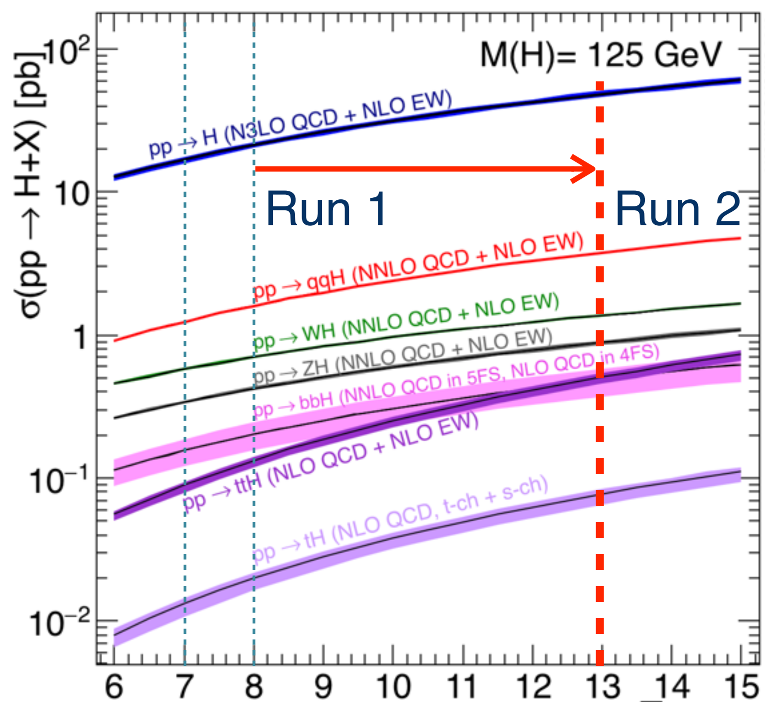

LHC Higgs XS WG Yellow Report 4

Stage 1 STXS framework

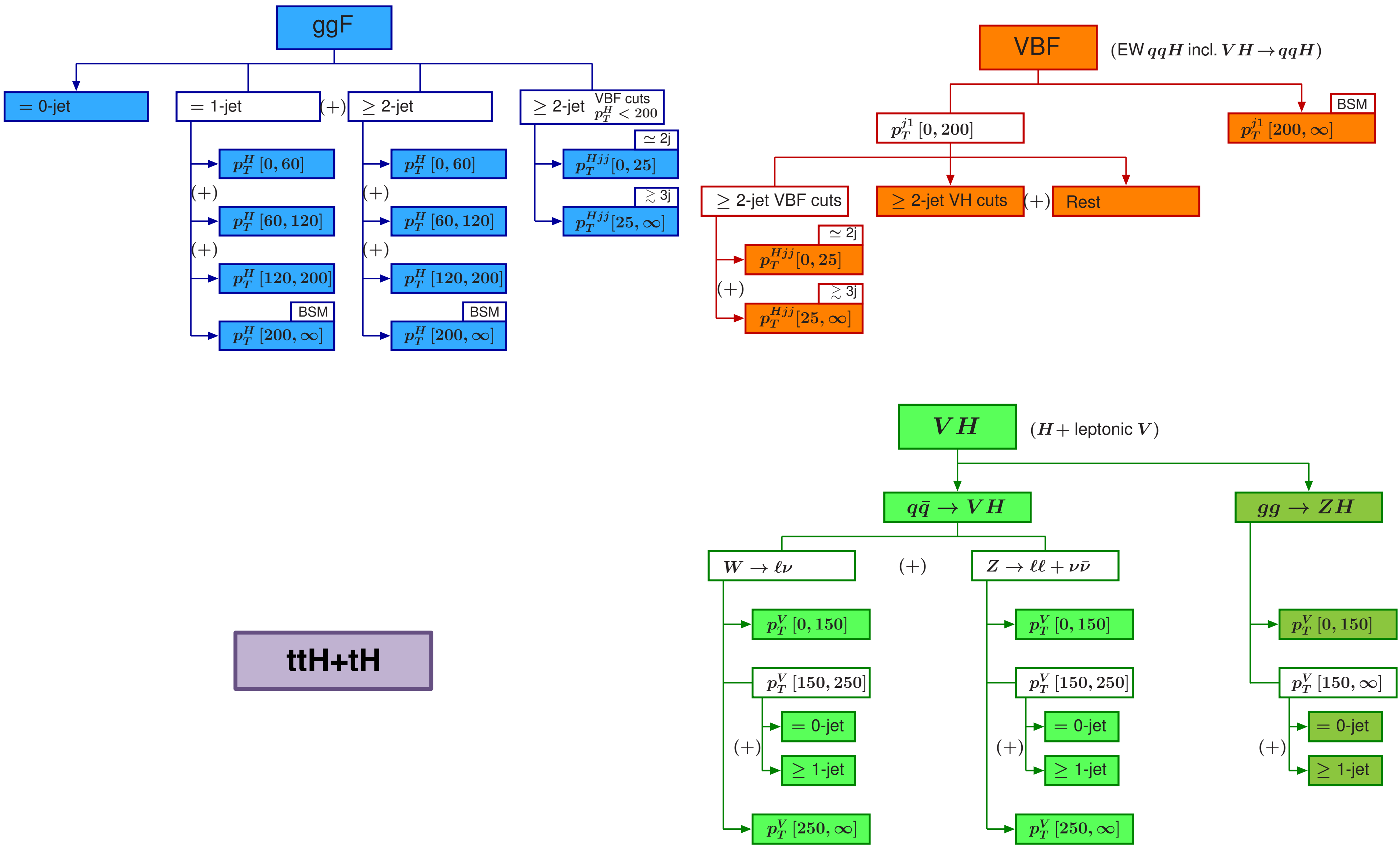

Stage 1.1 STXS framework

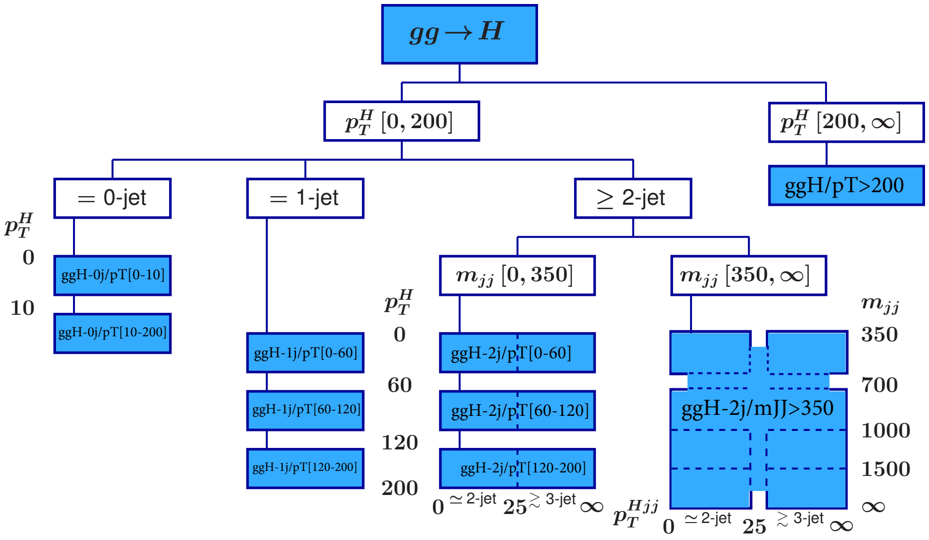

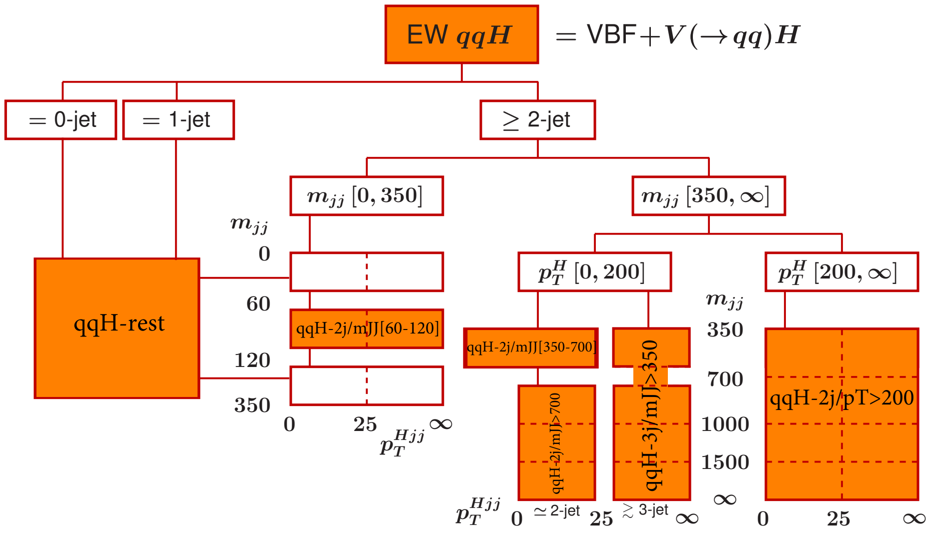

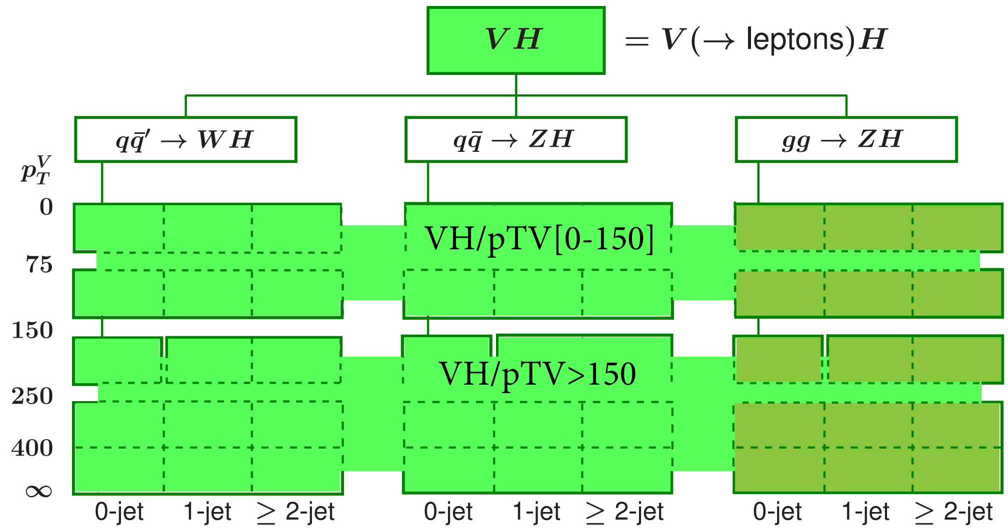

ttH+tH

H→γγ: signal fractions

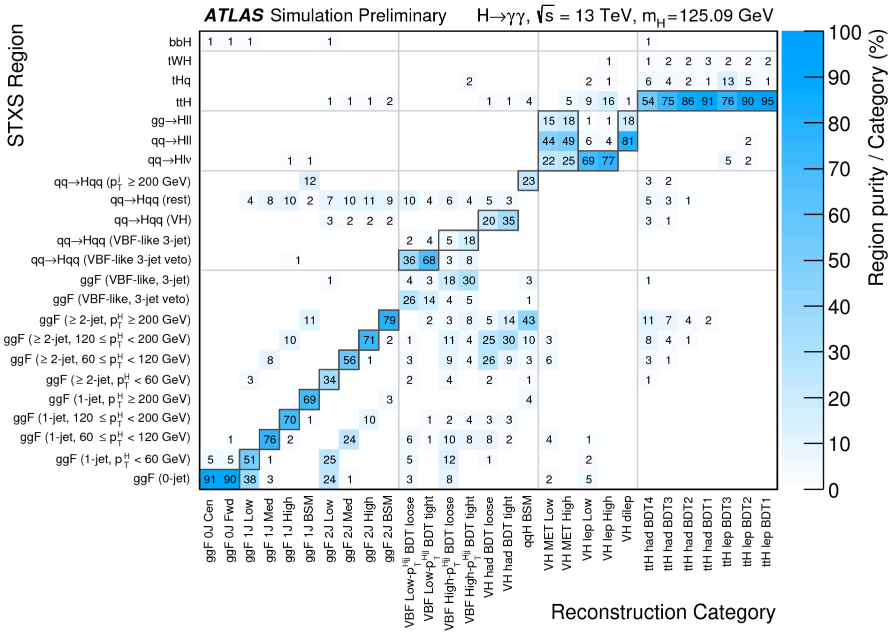

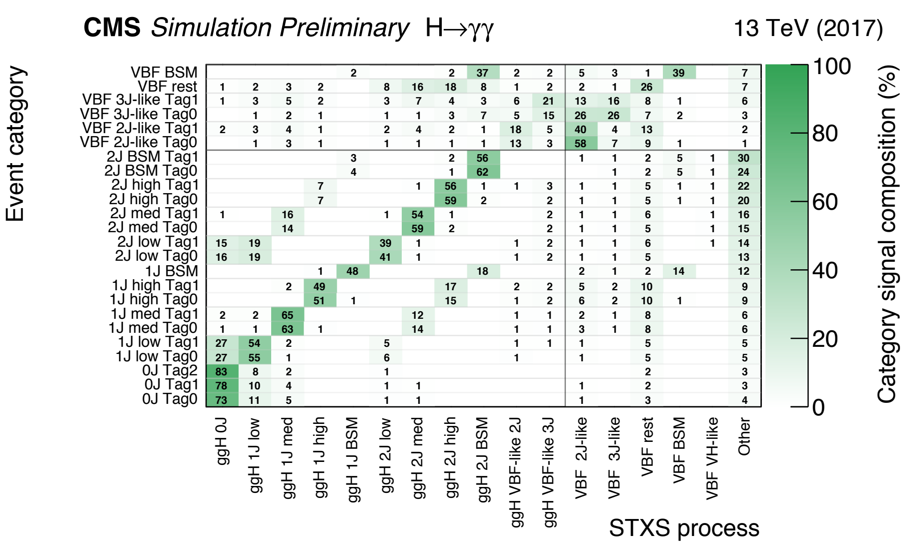

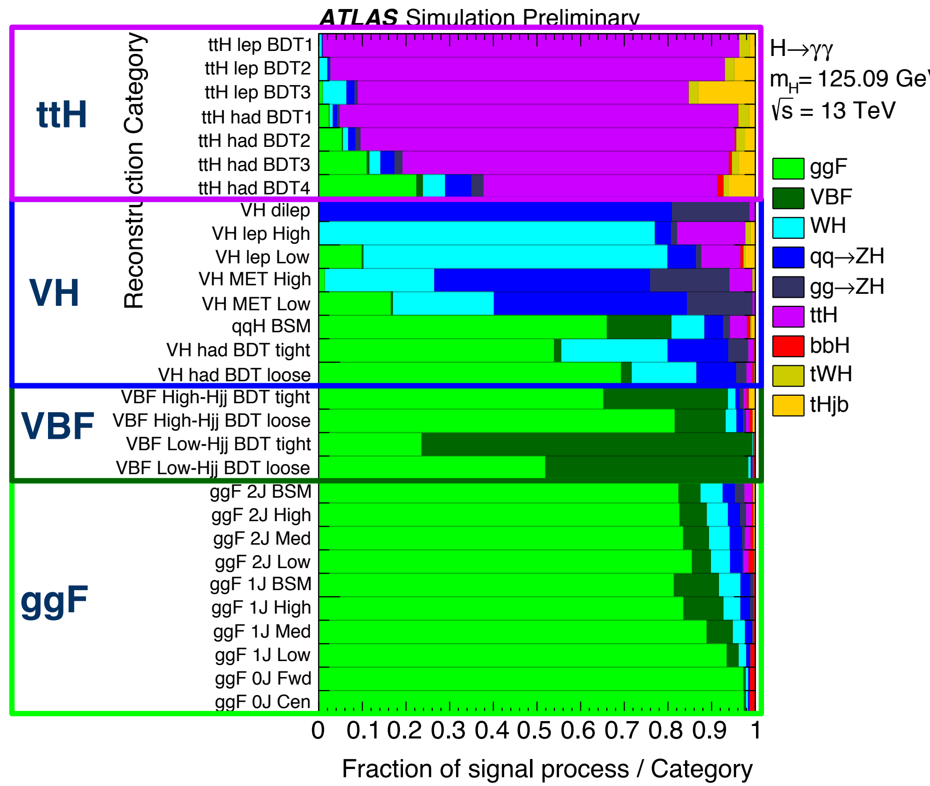

H→γγ: correlation matrices for STXS

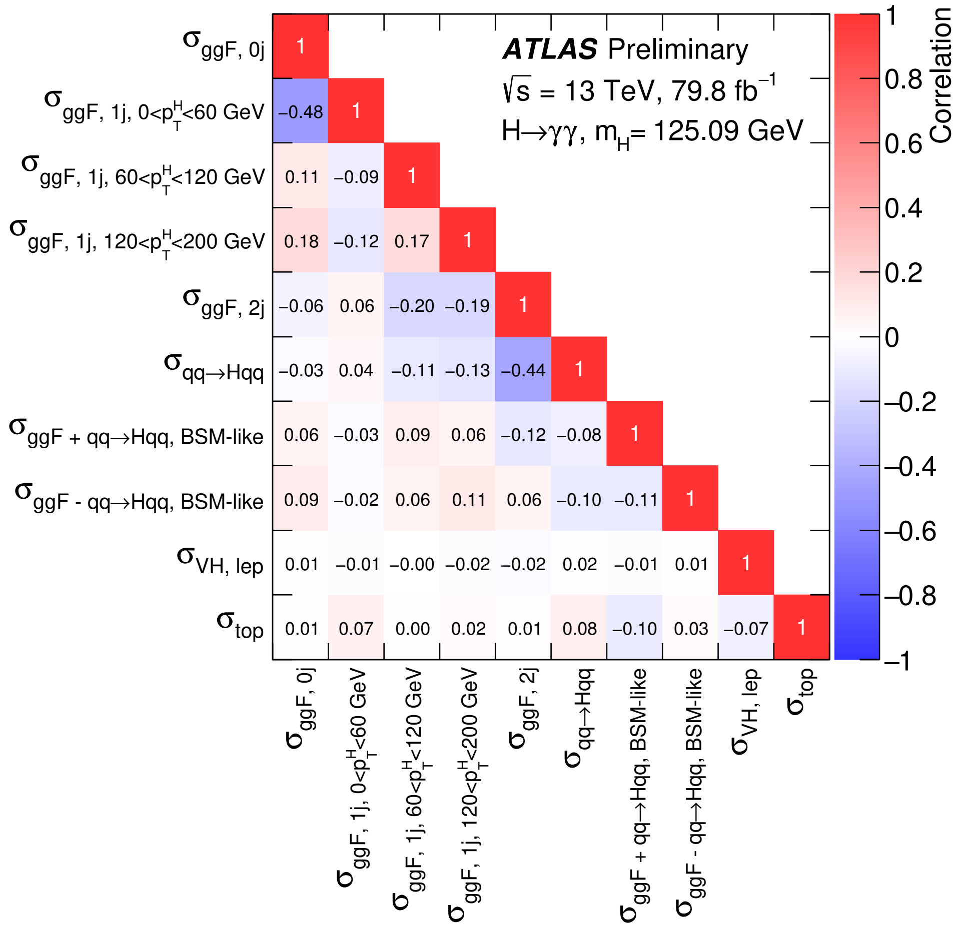

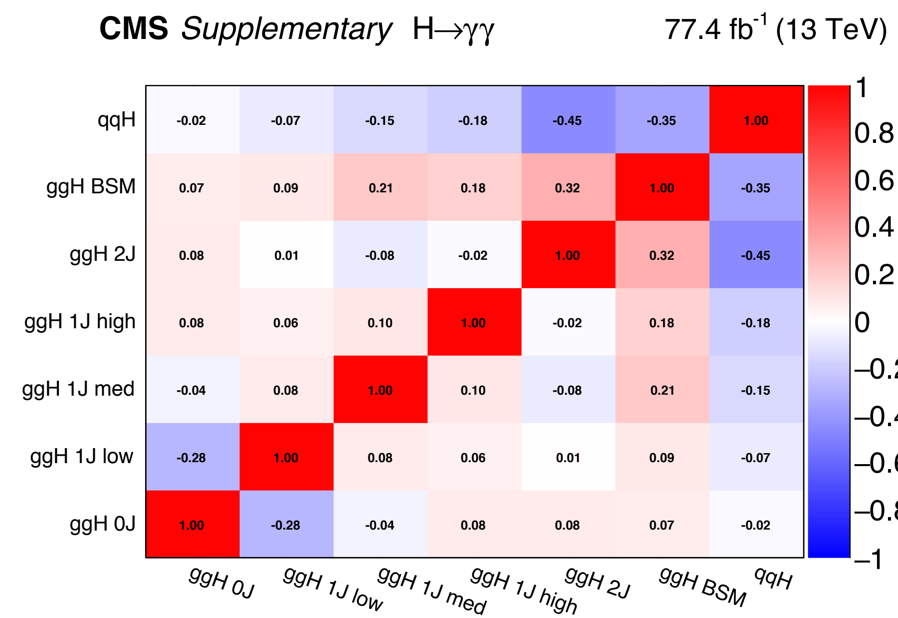

H→ZZ→4l: signal fractions

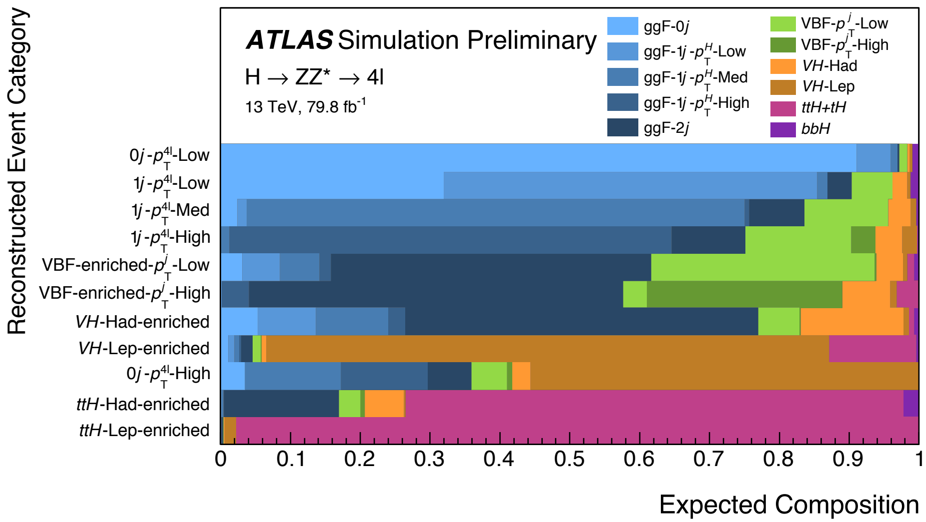

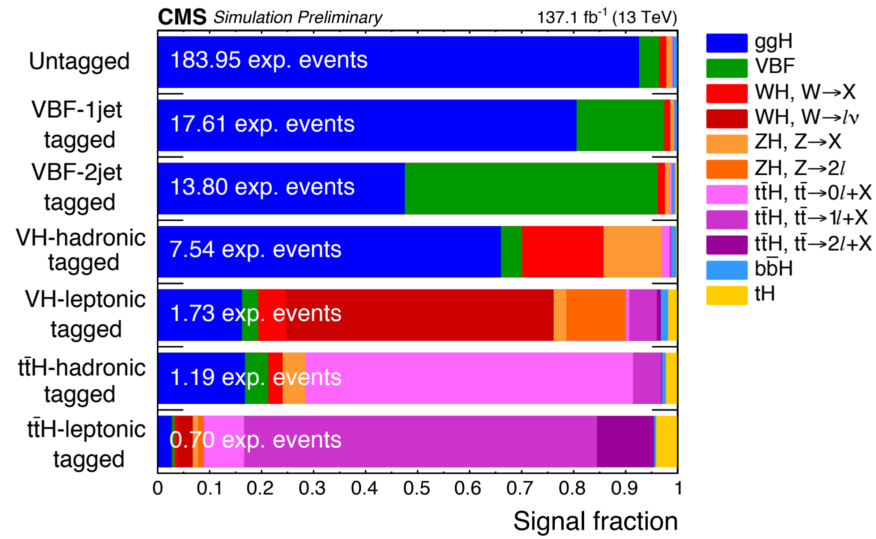

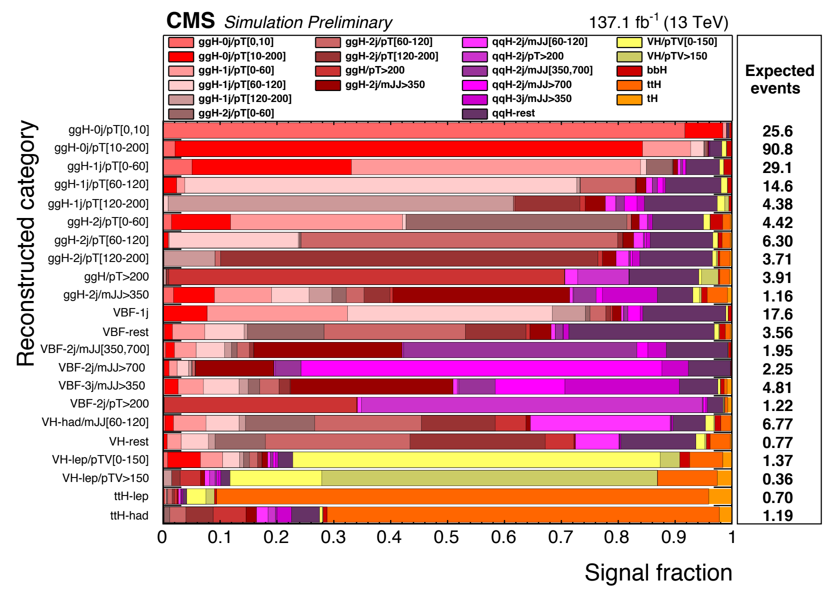

H→ZZ→4l: correlation matrices for STXS

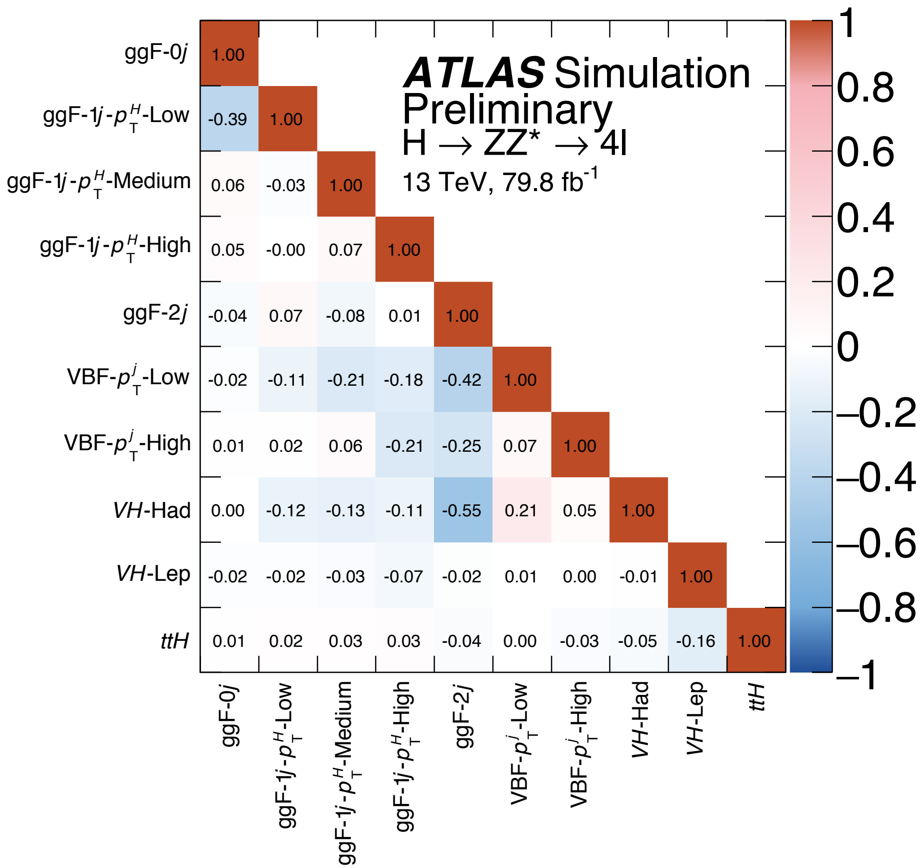

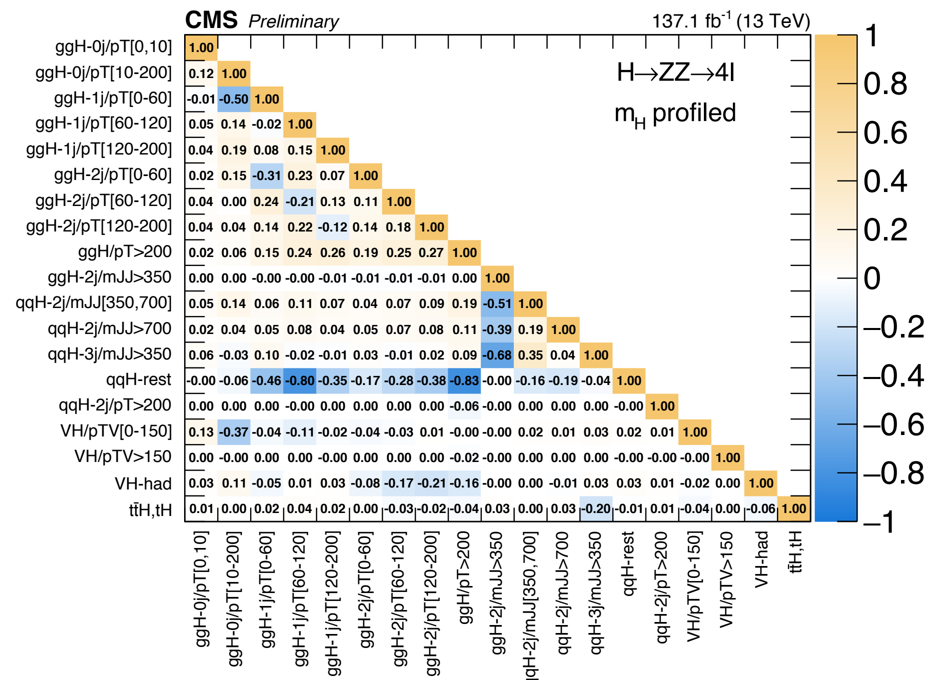

H→Zγ/γγ*→llγ

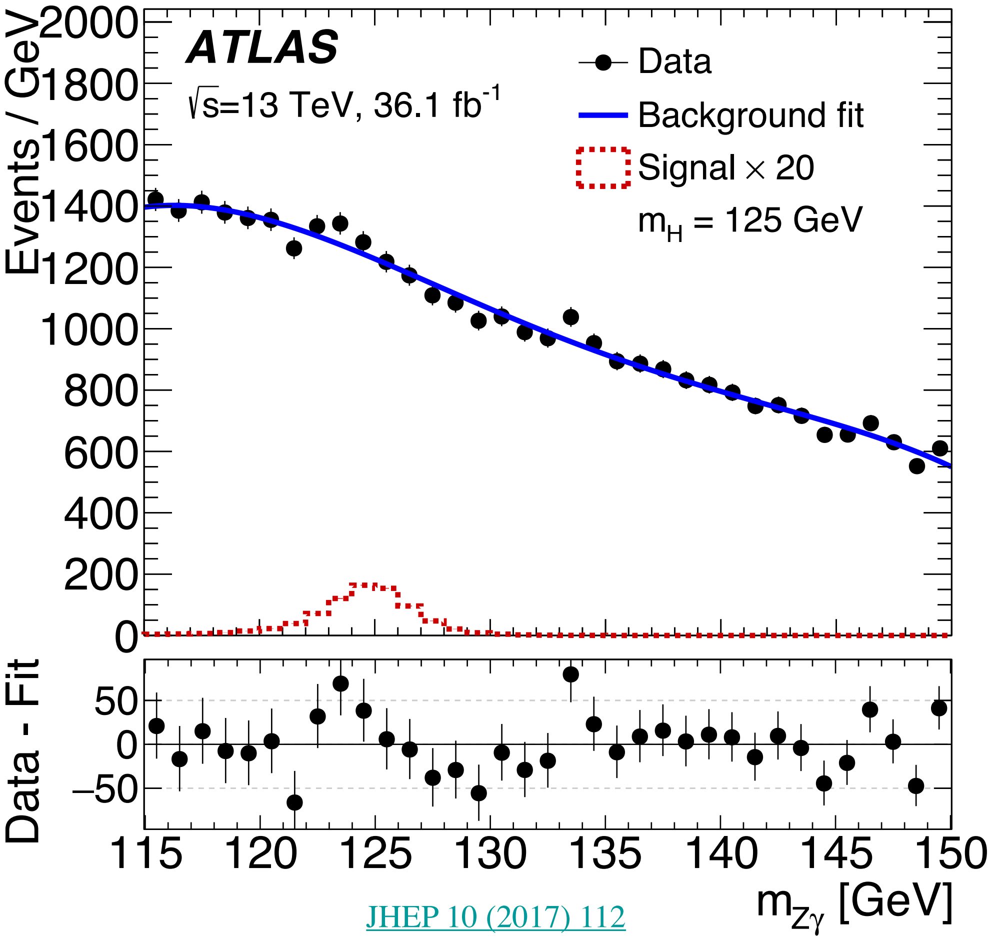

JHEP 10 (2017) 112

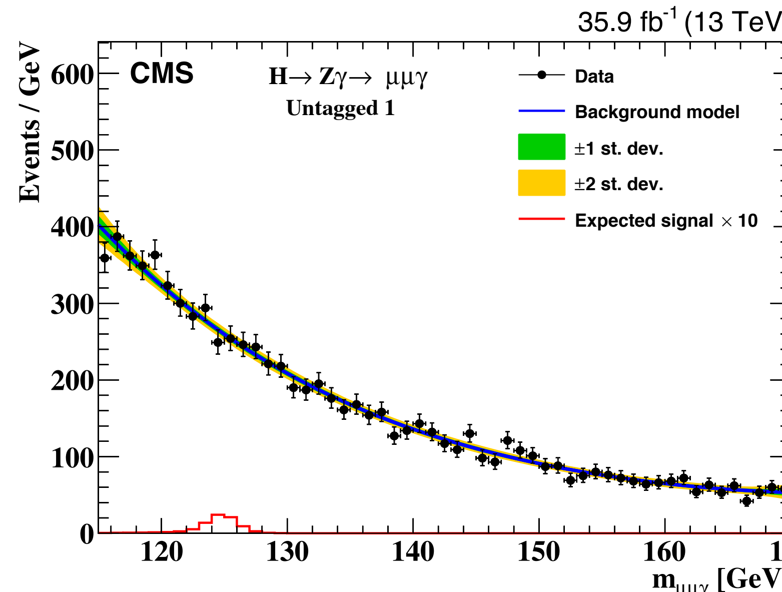

JHEP 11 (2018) 152

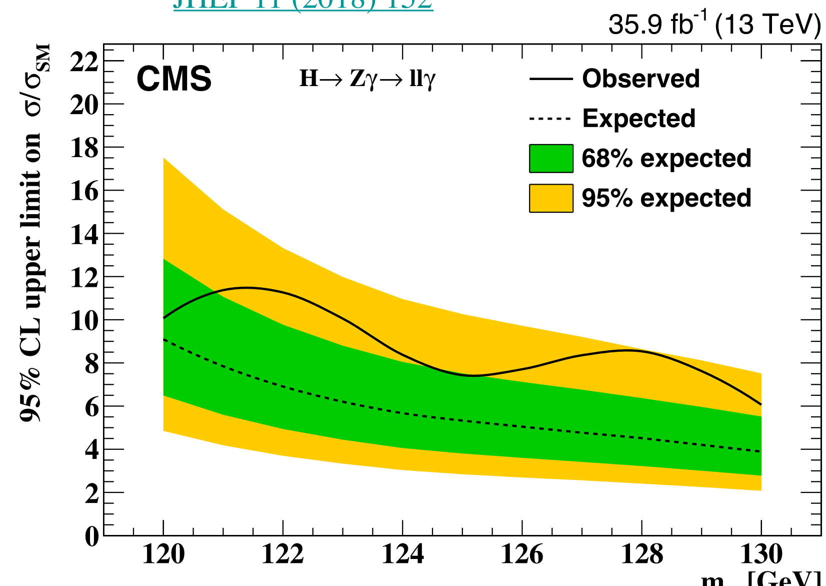

95% CL limit	Obs. [×SM]	Exp. [×SM]
ATLAS (Zγ)	6.6	5.2
CMS (Zγ+γγ*)	3.9	2.0

Prospect for off-shell constraint on Γ_H

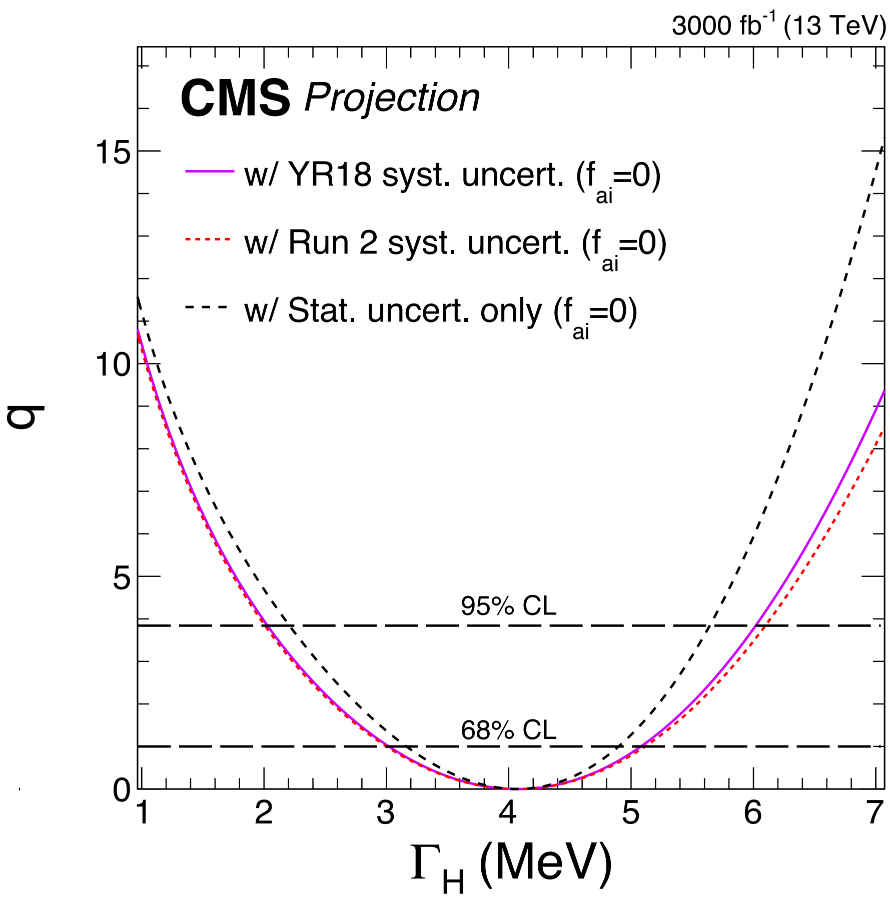

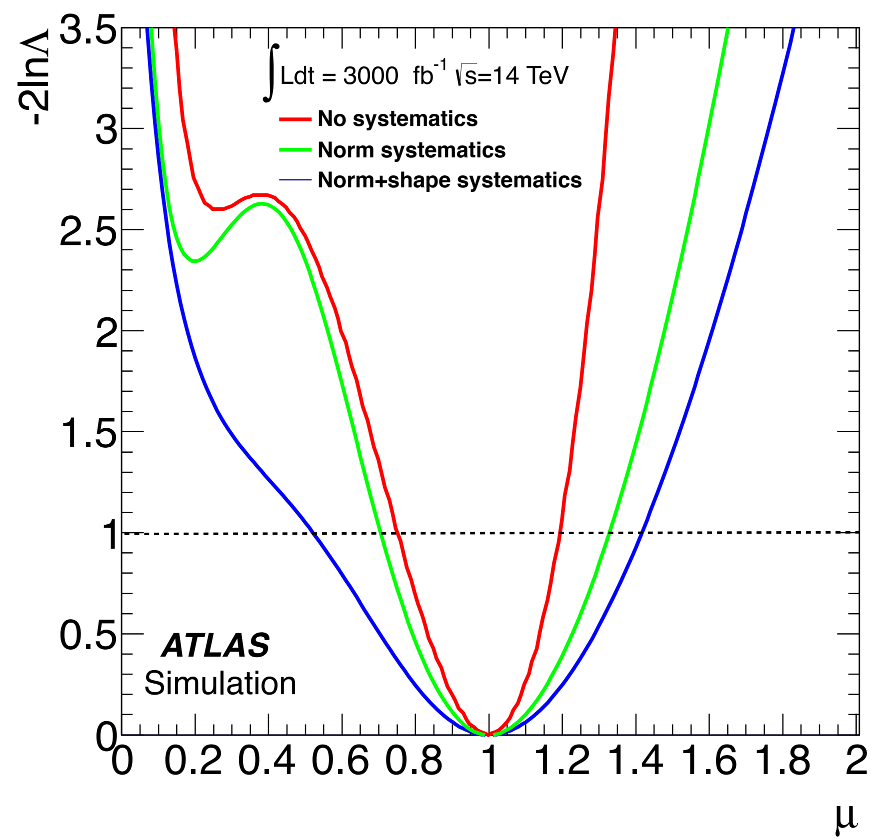

Theory model for HVV anomalous coupling studies

CMS:

$$A \sim \left[a_1^{VV} - \frac{\kappa_1^{VV} q_1^2 + \kappa_2^{VV} q_2^2}{\left(\Lambda_1^{VV}\right)^2} - \frac{\kappa_3^{VV} (q_1 + q_2)^2}{\left(\Lambda_Q^{VV}\right)^2} \right] m_{V1}^2 \epsilon_{V1}^* \epsilon_{V2}^* + a_2^{VV} f_{\mu\nu}^{*(1)} f^{*(2)\,\mu\nu} + a_3^{VV} f_{\mu\nu}^{*(1)} \tilde{f}^{*(2)\,\mu\nu}$$

ATLAS:

$$\begin{aligned}
\mathcal{L}_0^V = \Big\{ & \kappa_{SM} \left[\frac{1}{2} g_{HZZ} Z_\mu Z^\mu + g_{HWW} W_\mu^+ W^{-\mu} \right] \\
& - \frac{1}{4} \left[\kappa_{Hgg} g_{Hgg} G_{\mu\nu}^a G^{a,\mu\nu} + \tan\alpha \, \kappa_{Agg} g_{Agg} G_{\mu\nu}^a \tilde{G}^{a,\mu\nu} \right] \\
& - \frac{1}{4} \frac{1}{\Lambda} \left[\kappa_{HZZ} Z_{\mu\nu} Z^{\mu\nu} + \tan\alpha \, \kappa_{AZZ} Z_{\mu\nu} \tilde{Z}^{\mu\nu} \right] \\
& - \frac{1}{2} \frac{1}{\Lambda} \left[\kappa_{HWW} W_{\mu\nu}^+ W^{-\mu\nu} + \tan\alpha \, \kappa_{AWW} W_{\mu\nu}^+ \tilde{W}^{-\mu\nu} \right] \Big\} X_0 .
\end{aligned}$$